

AHMAD SHAHIR MOHAMAD

B. ENG. (HONS) ELECTRICAL AND ELECTRONIC

JANUARY 2015

**MODELING AND SIMULATION OF MODAL ANALYSIS-BASED
TECHNIQUE ON DISTRIBUTION/UTP NETWORK TO
EVALUATE THE HARMONIC RESONANCE**

AHMAD SHAHIR BIN MOHAMAD

ELECTRICAL AND ELECTRONIC ENGINEERING

UNIVERSITI TEKNOLOGI PETRONAS

JANUARY 2015

**Modeling and Simulation of Modal Analysis-Based Technique on Distribution/UTP
Network to Evaluate the Harmonic Resonance**

by

Ahmad Shahir Bin Mohamad

15030

Dissertation submitted in partial fulfilment of

the requirements for the

Bachelor of Engineering (Hons)

(Electrical and Electronics)

JANURARY 2015

Universiti Teknologi PETRONAS

Bandar Seri Iskandar

31750 Tronoh

Perak Darul Ridzuan

CERTIFICATION OF APPROVAL

Modeling and Simulation of Modal Analysis-Based Technique on Distribution/UTP Network to Evaluate the Harmonic Resonance

by

Ahmad Shahir bin Mohamad

15030

A project dissertation submitted to the
Electrical and Electronics Programme
Universiti Teknologi PETRONAS
in partial fulfilment of the requirement for the
BACHELOR ENGINEERING (Hons)
(ELECTRICAL AND ELECTRONICS)

Approved by,

(Khairul Nisak bt Md Hasan)

FYP Supervisor

UNIVERSITI TEKNOLOGI PETRONAS

TRONOH, PERAK

January 2015

CERTIFICATION OF ORIGINALITY

This is to certify that I am responsible for the work submitted in this project, that the original work is my own except as specified in the references and acknowledgements, and that the original work contained herein have not been accepted for any degree and is not concurrently submitted in candidature of any other degree.

(AHMAD SHAHIR BIN MOHAMAD)

ABSTRACT

Harmonic resonance had been regarded as one of the major problem in power quality issues. Numerous techniques had been deployed to reduce the effects of harmonic resonance in power system network. Of course installing harmonic filters is one of the techniques to mitigate the effect of harmonics but the concern in identifying the participating buses or network components that actually causing the harmonic resonance is not easy. Harmonic resonance mode analysis had been introduced to counter this arising issue. This technique had been tested, used and enhanced in order to improve the drawback of the commonly used frequency scan analysis technique. Under this technique, the results in terms of identifying the participating buses had been promising and reliable enough to be used as a reference to identify the best location to observe or excite harmonic resonance. Throughout this study, this technique will provide the necessary information regarding the participating buses that causing the harmonic resonance in several test system which include a part of Universiti Teknologi PETRONAS distribution network which is the new academic building. Through that information, further analysis can be made to identify the observability and the excitability of resonance through mode analysis.

ACKNOWLEDGEMENTS

All praise to Him, the most gracious and the most merciful for lending me the courage and determination to complete this project with success. I would like to express special thanks and gratitude to:

- My supervisor, Mdm Khairul Nisak bt Md Hasan for her continuous support, critics, ideas, guidance and contribution in succeeding this project
- UTP maintenance staff especially to Ir Mohd Fatimie Irzaq Khamis and Mr Rohaizan M. Ali Piah for their contribution in sharing knowledge and ideas
- Family members for continuous support and moral boost.
- Fellow colleagues for their support, knowledge, ideas and time spent during these whole period of studying in UTP

I shall always remember the good deeds till the end of my life. Thank you.

TABLE OF CONTENTS

CERTIFICATION	i
ABSTRACT	iii
ACKNOWLEDGEMENTS	iv
LIST OF TABLES	vi
LIST OF FIGURES	vii
CHAPTER 1:	INTRODUCTION	1
	1.1	Background of Study	1
	1.2	Problem Statement	2
	1.3	Objectives and Scope of Study	2
CHAPTER 2:	LITERATURE REVIEW & THEORY	3
	2.1	Fundamental of Harmonic Resonance	3
	2.2	Case Studies on Harmonic Analysis	4
CHAPTER 3:	METHODOLOGY/ PROJECT WORK	7
	3.1	Methodology	7
	3.2	Project Key Milestone.	10
	3.3	Project Timeline (Gantt chart)	10
CHAPTER 4:	RESULTS & DISCUSSION	11
CHAPTER 5:	CONCLUSION & RECOMMENDATION	41
REFERENCES	43
APPENDICES	45

LIST OF TABLES

Table 1	Modal Analysis Results of the Three Bus Test System .	13
Table 2	Five bus test system transmission line parameters [p.u.] .	15
Table 3	Five bus test system fundamental frequency power flow [p.u.]	16
Table 4	Five bus test system load impedance at node 3, 4 and 5 based on CIGRE’s load model (iii)	16
Table 5	Modal Analysis Results of the Five Bus Test System .	18
Table 6	Load flow result for the standard IEEE 14 Bus Test system .	21
Table 7	Modal Analysis Results for the Standard IEEE 14 Bus Test System	25
Table 8	Modal Analysis Results for the Modified IEEE 14 Bus Test System	28
Table 9	Modal Analysis Results for the Modified IEEE 14 Bus Test System (continued)	29
Table 10	Summary of the modal results on the modified IEEE 14 bus network	30
Table 11	Load flow results for UTP new academic building network .	32
Table 12	Resonance mode information on UTP new academic building network (Mode 15)	34
Table 13	Resonance mode information on UTP new academic building network (Mode 16)	38
Table 14	Resonance mode information on UTP new academic building network (Mode 17)	39
Table 15	Summary of the modal results on the UTP new academic building network	40

LIST OF FIGURES

Figure 1	General flow of the author’s project methodology	9
Figure 2	Three bus test system	11
Figure 3	Frequency Scan Analysis Results of the Three Bust Test System.	12
Figure 4	Modal Impedances of the Three Bus Test System	12
Figure 5	Five bus test system with SVC	15
Figure 6	Frequency Scan Analysis Results of the Five Bust Test System	17
Figure 7	Modal Impedances of the Five Bust Test System	17
Figure 8	Standard IEEE 14 Bus Test System	20
Figure 9	Frequency Scan Analysis of the Standard IEEE 14 Bus Test System.	24
Figure 10	Harmonic Resonance Mode Analysis of the Standard IEEE 14 Bus Test System.	24
Figure 11	Frequency Scan Analysis for the Modified IEEE 14 Bus Test System	27
Figure 12	Harmonic Resonance Mode Analysis of the Modified IEEE 14 Bus Test System	27
Figure 13	Simplified single line diagram for UTP new academic building network	33
Figure 14	Frequency Scan Analysis of UTP new academic building network	36
Figure 15	Harmonic Resonance Mode Analysis for UTP new academic building network	36

CHAPTER 1

INTRODUCTION

1.1 BACKGROUND OF STUDY

Harmonics have existed since the early days of the introduction of alternating current. In general definition, harmonics can be referred to the frequency components of a time-varying signal. In electrical power system, harmonics can rather be defined as a sinusoidal waveform with frequency that has integral multiple of fundamental frequency, mostly at 60Hz. Harmonics are mostly produced by non-linear loads. Due to the various kinds of non-linear loads, the level of harmonics produced varied and can somehow affect the seriousness of the harmonics impact. The network operating conditions as well as the interaction between passive components such as capacitors, inductors and resistors aggravate the effects even more. At some frequencies, these passive components can react with each other to create what is called the resonance condition.

There are two types of resonance that frequently occur in electrical power system which are series and parallel resonance. Series resonance gives rises to harmonic current while parallel resonance causes amplification to voltage disturbance. As resonance can happen at certain frequencies, it would be acute if it occurs at the same frequency as the harmonics produced by the loads. Hence, all possible resonances need to be aware and taken care of in designing and installing power factor correction capacitors or any other equipment.

1.2 PROBLEM STATEMENT

As mentioned in the earlier section, resonance can be severe if it occurs at the same frequency as the harmonics introduced by the loads. Thus, solutions to overcome the effects of resonance need to be implemented. One of the solutions is by the installation of harmonic filters. However, in a distribution network, both reactive compensation devices and other shunt capacitance element exist. Hence, the main problem would be the difficulty in making decision on installing harmonic filters, which if not properly installed, can affect its effectiveness in mitigating harmonics.

In order to decide on the optimum location for harmonic filter installation, a method need to be used which can assist in identifying the participating buses or elements that produces harmonics. To date, research has shown that there are techniques to evaluate the resonance in the system. One of them is the harmonic resonance mode analysis. However, it is not fully known that this method can be effective enough compared to the other available methods as this is a relatively new method. Hence, the second problem arises which is the challenge in using this relatively new method in evaluating the harmonics in the system, which is for this project, the UTP distribution network.

1.3 OBJECTIVES AND SCOPE OF STUDY

The main objective of this project can be stated as follows:

- To implement the harmonic resonance mode analysis technique on several test system
- To model and simulate UTP new academic building using MATLAB software utilizing real parameters and data

Harmonic resonance study is related to power systems, which compliance with what the author is majoring currently in the Power System major for Final Year semester in Electrical and Electronics Engineering course. Hence, this project is concluded to be feasible enough based on the scope of Electrical and Electronic Engineering and the time frame provided which is until the end of Final Year Project II (FYP II).

CHAPTER 2

LITERATURE REVIEW & THEORY

2.1 FUNDAMENTAL OF HARMONIC RESONANCE

As been described previously, harmonics can be severe and can cause serious problems if not treated properly. Considerable efforts have been put into account in solving this issue which affects largely in power quality issues. As mentioned in [1], devices that involve electronic switching and have nonlinear voltage and current relationships can be regarded as the main cause of harmonics. These devices such as personal computers (PCs) and televisions (TVs) create concerns in power quality issues. With the addition of other harmonic-generating loads throughout the power network, even the interference with control, communication and protective equipment [2] had become one of the raising issues in electrical power industry. Another raising issue that becomes a major debate in power quality includes the resonance issue.

In a study of mitigating harmonic resonance through modal analysis [3], resonance can be resulted from the exchange of reactive power between capacitive and inductive elements at a specific frequency. In electrical power systems, there are two types of resonance which are parallel and series resonance. Both parallel and series resonance can cause harmful effects, in which the former causes rises to the amplification of voltage disturbance, while the latter produces high and undesired harmonic currents [4]. In a power system network, the components and devices are generally comprised of both inductive and capacitive components [5]. Due to power factor correction and voltage support, the application of capacitive elements such as shunt capacitors and capacitor banks were introduced, which consequently created numerous complex circuits made up

of series and parallel connected inductive and capacitive elements [6]. At certain harmonic frequencies, series and parallel harmonic resonances will occur depending on the level of injection of the harmonic resources.

2.2 CASE STUDIES ON HARMONIC ANALYSIS

Despite the severe consequences of harmonics, there are different methods or harmonic analysis techniques that can be implemented in both frequency and time domain [7] in order to study the initiation and transmission of harmonics. Harmonic analysis is necessary to be conducted in distribution system to analyse the equipment or network component so that optimal location for harmonic filter installation can take place [8]. Many of these techniques describe their own specific method in identifying the harmonic frequency and existence of harmonics but the only practical and applicable method at present is probably the frequency scan analysis [9][10].

Frequency scan analysis calculates the driving point impedance of the bus where the one p.u. of current injection occurs. Large impedance at certain frequencies indicates harmonic resonance. However, despite its ability to detect and reveal the existence of harmonics, it could not provide specific information on which network components had actually caused the resonance and the best location to place harmonic filters to mitigate the problems [11].

Nevertheless, the existence of the harmonic resonance mode analysis had somehow help to solve the problem through the ability to detect the potential of harmonic resonance as well as the impacts of numerous network elements towards a resonance [12]. In this method, the complexity and ways to determine which location where modal resonance occur the most are investigated. The resonance characteristics are determined from eigenvalue interpretation. Through the decomposition of admittance matrix into left and right eigenvector matrices as well as diagonal eigenvalue matrix, the excitability and observability of a particular mode can be identified. Excitability means the tendency of the buses to create or cancel harmonics while observability means the ability to observe the resonance of a particular mode. Right eigenvector holds the responsibility in giving

the information on the excitability while left eigenvector gives information on the observability. The combination or product of these two eigenvectors forms a participation factor which reveals the location which is the easiest to observe and excite harmonic resonance.

Equation (1) shows the decomposition of admittance matrix into right and left eigenvector matrices with its diagonal eigenvalue matrix, as stated in [13]. From here, it can be understood that the right and left eigenvector values can be combined to form the participation factor as shown in equation (2).

$$[Y] = [L][\Lambda][T] \quad (1)$$

$$\begin{aligned} [V] &= [L][\Lambda]^{-1}[T][I] = [L] \begin{bmatrix} \lambda_1^{-1} & 0 & 0 & 0 \\ 0 & \lambda_2^{-1} & 0 & 0 \\ 0 & 0 & \dots & 0 \\ 0 & 0 & 0 & \lambda_n^{-1} \end{bmatrix} [T][I] \\ &= \begin{bmatrix} L_{11} & L_{12} & \dots & L_{1n} \\ L_{21} & L_{22} & \dots & L_{2n} \\ \dots & \dots & \dots & \dots \\ L_{n1} & L_{n2} & \dots & L_{nn} \end{bmatrix} \begin{bmatrix} \lambda_1^{-1} & 0 & 0 & 0 \\ 0 & 0 & 0 & 0 \\ 0 & 0 & \dots & 0 \\ 0 & 0 & 0 & 0 \end{bmatrix} \begin{bmatrix} T_{11} & T_{12} & \dots & T_{1n} \\ T_{21} & T_{22} & \dots & T_{2n} \\ \dots & \dots & \dots & \dots \\ T_{n1} & T_{n2} & \dots & T_{nn} \end{bmatrix} [I] \\ &= \begin{bmatrix} \lambda_1^{-1}L_{11} & 0 & \dots & 0 \\ \lambda_1^{-1}L_{21} & 0 & \dots & 0 \\ \dots & \dots & \dots & \dots \\ \lambda_1^{-1}L_{n1} & 0 & \dots & 0 \end{bmatrix} \begin{bmatrix} T_{11} & T_{12} & \dots & T_{1n} \\ T_{21} & T_{22} & \dots & T_{2n} \\ \dots & \dots & \dots & \dots \\ T_{n1} & T_{n2} & \dots & T_{nn} \end{bmatrix} [I] \\ &= \lambda_1^{-1} \begin{bmatrix} L_{11}T_{11} & L_{11}T_{12} & \dots & L_{11}T_{1n} \\ L_{21}T_{11} & L_{21}T_{12} & \dots & L_{21}T_{1n} \\ \dots & \dots & \dots & \dots \\ L_{n1}T_{11} & L_{n1}T_{12} & \dots & L_{n1}T_{1n} \end{bmatrix} \begin{bmatrix} I_1 \\ I_2 \\ \dots \\ I_n \end{bmatrix} \quad (2) \end{aligned}$$

where,

[Y] = admittance matrix,

[L] = left eigenvector matrix

[R] = right eigenvector matrix

[\Lambda] = diagonal eigenvalue matrix

From (2) also, it can be seen that if the eigenvalue, λ_1 is very small or equals to 0, the relatively inverse eigenvalue, λ^{-1}_1 will be eventually very high, which will causes the modal voltage at mode 1 to be very high. However, this will not affect other modal voltage as there is no ‘mutual integration’ or ‘coupling’ with the mode 1 current. This is what makes this method seems easy in identifying the location of the resonance in a particular matrix form through eigenvalue interpretation even though the computation and the complexity might be a bit harder compared to the frequency scan analysis method.

CHAPTER 3

METHODOLOGY/ PROJECT WORK

3.1 METHODOLOGY

In order to achieve the objective of this study, the author has conducted a proper planning and methodology. The author firstly conducted detailed preliminary researches on the frequency scan analysis technique as well as the harmonic resonance mode analysis technique. Upon completing the research, the author moved on into building the algorithm for both techniques in MATLAB software. Once the algorithm is made, the author tested the algorithm on several test system, which includes three bus test system, five bus test system as well as both IEEE standard and modified 14 bus test system. The raw data are basically obtained from research papers for different test systems. Upon completion, the results are recorded which consists of a frequency versus impedance graph for both technique. Detailed analysis and discussion are made based on the results obtained.

As soon as the author completed the test on all the test system, the preparation of obtaining the UTP network data has already begun. In order to obtain all the necessary data, a few meetings with the UTP maintenance team need to be conducted. The author has conducted a few field trips to understand in detail on the schematic and layout of UTP new academic building network. Some images are captured and can be viewed in the Appendix section. From the meetings also, it was acknowledged that there were not so many data and research on harmonics-related problem as there were no raising issues or concern regarding harmonics in UTP. This is due to the large neutral cable on the generator side, which prevents the severe effects and consequences of harmonics.

Hence, little concern was given in harmonic issues unless the problem rises which involves serious effects throughout the entire distribution network.

Once the data are retrieved, the load flow study is performed. For a larger network, it is essential to undergo load flow study to investigate the real and reactive power flow as well as the bus voltage profiles. To perform the load flow study, the author used a toolbox that can be linked to the MATLAB software called PSAT toolbox. PSAT which stands for Power System Analysis Toolbox functions as a medium to analyze and simulate power system problems/scenarios utilizing the help of graphical user interface (GUI). It enables the users to undergo various tests on electrical power system network including load flow analysis, stability analysis and many more.

For this project, some of the test system such as the three bus test system did not need to perform the load flow test as it comprises of a single connected load. Hence, by utilizing the values directly from the research papers, this step can be skipped and proceed to the next step which is the simulation of harmonic resonance. Once the load flow for the UTP new academic building network has been performed, the algorithm is used to simulate the resonance in the network and the results are obtained. Again, detailed analysis and discussion are made and some suggestion and recommendation for future researches are also presented.

Figure 1 shows the methodology conducted by the author throughout the FYPI and FYPII period.

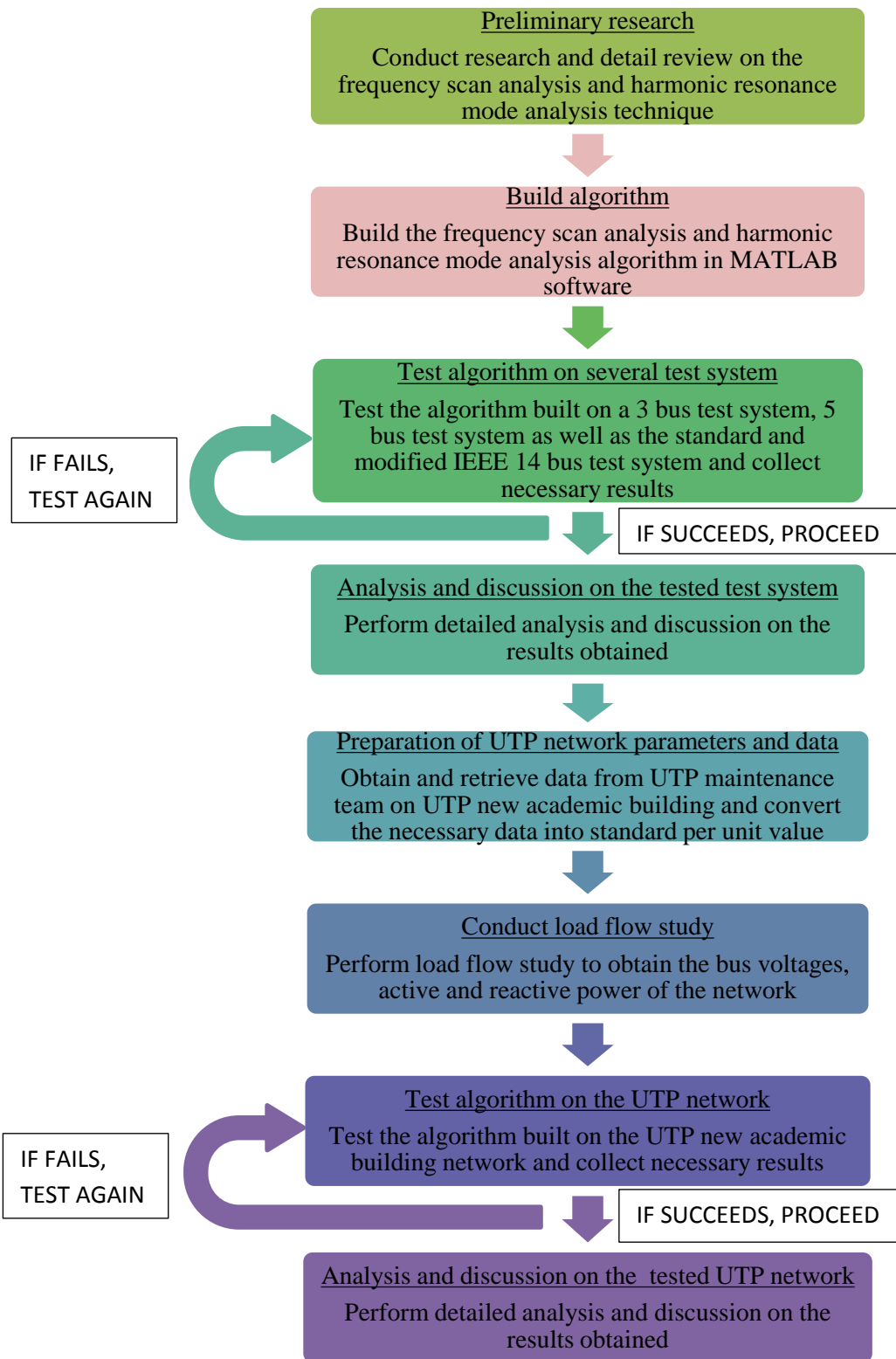


FIGURE 1. General flow of the author's project methodology

3.2 PROJECT KEY MILESTONE

In order to be able to complete the project within the time frame given by the Final Year Project committee, a key milestone was developed to keep track on the project objective, data, research studies, development, and compilation of final Final Year Project report. The key milestone can be viewed in Appendices section.

3.3 PROJECT TIMELINE (GANTT CHART)

For more detailed schedule on the Final Year Project development, the author has developed a Gantt chart to keep track on more detail actions that need to be taken to ensure the timeline of the key milestone is followed.

Please refer to the Appendices section for the author's project timeline or Gantt chart that will be used as the main reference for Final Year Project I and II.

CHAPTER 4

RESULTS AND DISCUSSION

For the author to get familiarize with the harmonic resonance mode analysis method, several test systems have been tested using the frequency scan analysis and the harmonic resonance mode analysis. The first test system is composed of three bus test system. The second test system is composed of five bus test system. The third and fourth test system composed of the IEEE 14 bus test system, the standard and modified one, respectively.

4.1 Three bus test system

The configuration for the three bus test system is taken from [12] as figure 2.

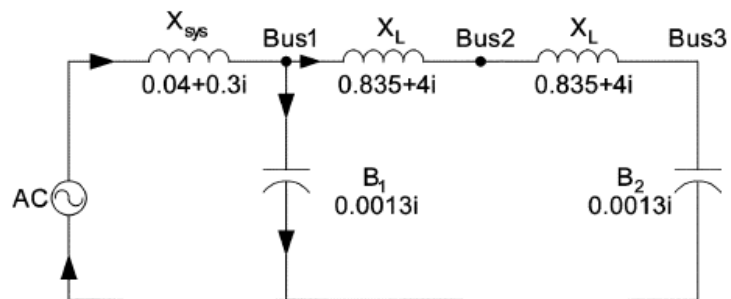


FIGURE 2. Three bus test system

The author purposely created both the frequency scan analysis code in Appendix section as well as the harmonic resonance mode analysis code to compare the differences and the effect of these two techniques on the expected impedance versus frequency graph. The result from this code is shown as in figure 3 and figure 4.

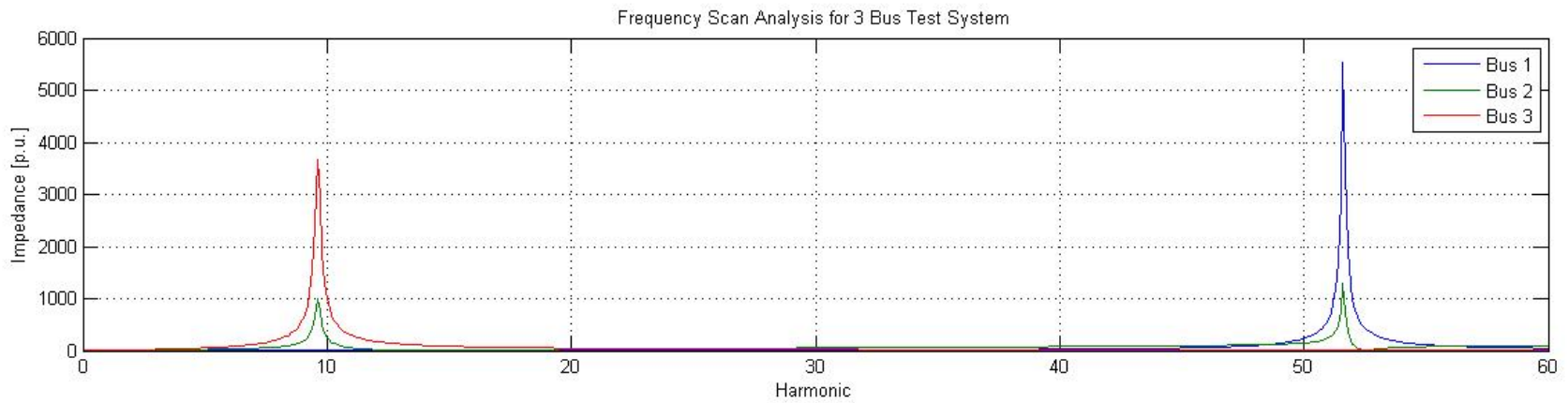


FIGURE 3. Frequency Scan Results of the Three Bus Test System

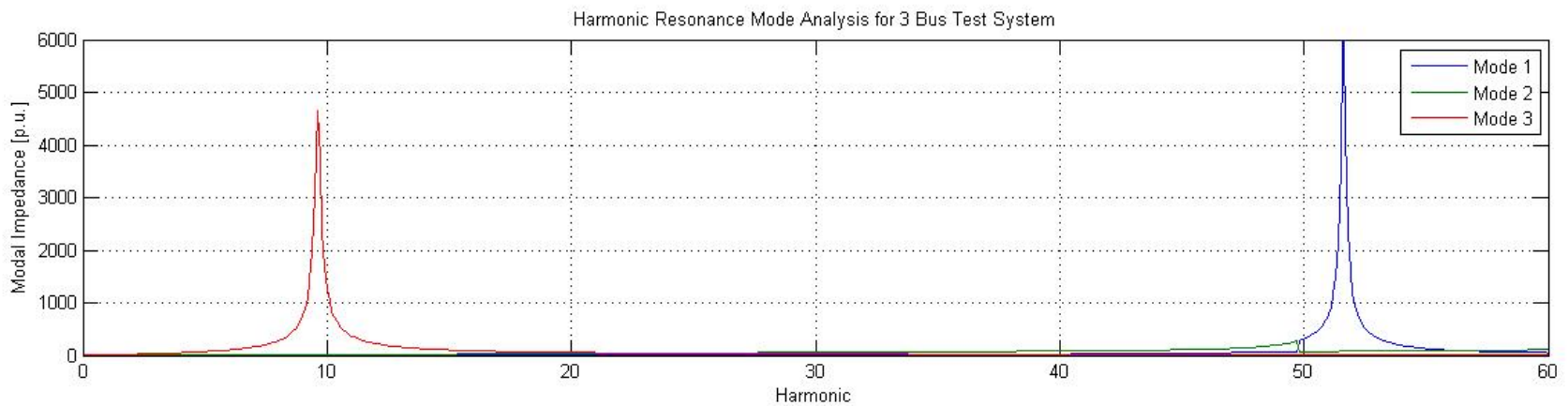


FIGURE 4. Modal Impedances of the Three Bus Test System

Based on the graphs obtained, there are some differences between the frequency scan analysis method and the harmonic resonance mode analysis method. Figure 4 shows that there are resonance phenomenons at all buses. At a resonance frequency of 9.6 p.u., it can be seen that bus 2 and bus 3 are experiencing resonance. Hence, it can be troublesome in recognizing the significance of each bus or which buses actually took part in the resonance condition at a specific frequency. Meanwhile, in Figure 4, the result reveals that there is only one resonance that actually occurring at each specific frequency. At a resonance frequency of 9.6 p.u., mode 3 has the highest modal impedance value (eigenvalue) while mode 1 gives a high modal impedance value at a resonance frequency of 5.6 p.u. These modes actually can be further analysed to determine the eigenvalue and eigenvector characteristics whereby the product of these eigenvalue and eigenvector can be known as the participation factor. This participation factor helps to determine which bus actually played a key role in producing the resonance condition.

Table 1 shows the value of the critical eigenvalue, eigenvectors and participation factor for each mode at their respective resonance frequency.

TABLE 1. Modal Analysis Results of the Three Bus Test System

Resonant frequency (p.u.)		9.6 (Mode 3)	51.6 (Mode 1)
Critical eigenvalue (D)		0.00021/-10.08°	0.00015/-10.45
Right eigenvector (R)	Bus 1	R31=0.0332/0.57°	R11=0.9016/-0.31
	Bus 2	R32=0.4605/0.15°	R12=0.4344/0.51
	Bus 3	R33=0.8870/-0.11°	R13=0.0338/-179.38
Left eigenvector (L)	Bus 1	L13=0.03323/0.68°	L11=0.9001/0
	Bus 2	L23=0.4605/0.26°	L21=0.4343/0.82
	Bus 3	L33=0.887/0°	L31=0.0338/-179.07
Participation factor (RxL in magnitude)	Bus 1	PF13=0.0011	PF11=0.8115
	Bus 2	PF23=0.2121	PF21=0.1887
	Bus 3	PF33=0.7868	PF31=0.0011

The results above reveal that the key participating buses for mode 1 at 51.6 p.u. is bus 1 while the key participating buses for mode 3 at 9.6 p.u. is bus 3. Theoretically, this can be proven through calculation using the basic formula in calculating the frequency at which the inductance and the capacitance are said to be equal.

Analysing the system from the largest participating factor, for bus 1, the resonance frequency can be computed as $f = \sqrt{Xc/Xsys} = 50.637$ while for bus 3, the resonance frequency is said to be $f = \sqrt{Xc/(Xsys + 2XL)} = 9.633$. Comparing the theoretical values with the experimental values obtained through the harmonic resonance mode analysis method, it can be concluded that the information and data produced by the modal analysis method can be reliable enough to identify which location is the best to excite or observe harmonic resonance condition.

Other than that, from the graphs obtained, it can be seen that the amplitude of the impedances in the frequency scan analysis method and the harmonic resonance mode analysis method are not the same. This is because the impedances shown in the graph of the frequency scan analysis is the actual physical impedance value whereby the impedance value in the graph of the harmonic resonance mode analysis is just the modal impedance value which have been mathematically influenced by the eigenvalue and the eigenvectors values. The modal impedance value can be calculated by inverting the value of the eigenvalue. Hence, it cannot be expected that the amplitude of the impedances will be the same for each test system. However, in some cases, there might be some possibilities that the actual or physical impedance can be the same or identical with the modal impedances. This will be proven in the next case of test system.

4.2 Five bus test system

The next test system is a five buses test system taken from [14] as shown in figure 5.

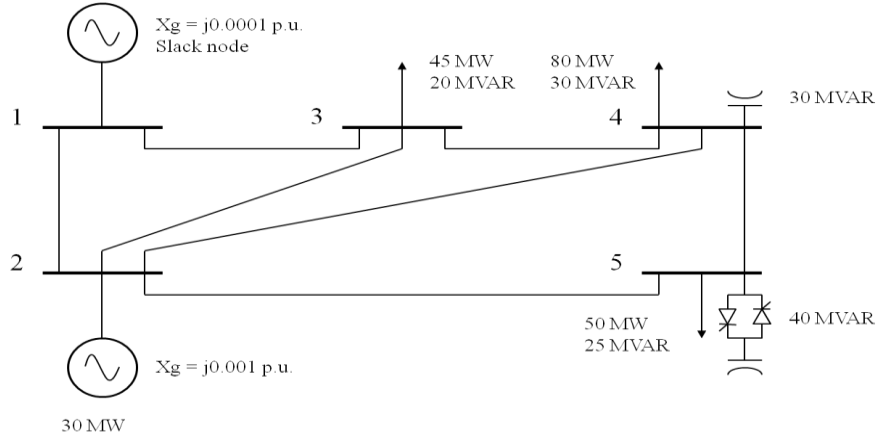


FIGURE 5. Five bus test system with SVC

A basic test system utilizing a static VAR compensator (SVC) connected at node 5 can be seen as in figure 5 above. From figure 5, it is then converted into a nominal pi-circuit based on CIGRE's load model (iii). The SVC is said to be delta connected and act as a constant harmonic current source. The transmission line parameters and its fundamental frequency power flow can be seen in table 2 and table 3, respectively.

TABLE 2. Five bus test system transmission line parameters [p.u.]

Line, $p-q$	Impedance, z_{pq}	Line charging, $y_{pq}/2$
1-2	$0.02+j0.06$	$0.0+j0.030$
1-3	$0.08+j0.24$	$0.0+j0.025$
2-3	$0.06+j0.18$	$0.0+j0.020$
2-4	$0.06+j0.18$	$0.0+j0.020$
2-5	$0.04+j0.12$	$0.0+j0.015$
3-4	$0.01+j0.03$	$0.0+j0.010$
4-5	$0.08+j0.24$	$0.0+j0.025$

TABLE 3. Fundamental frequency power flow [p.u.]

Node	V	θ	Pg	Qg	Pd	Qd
1	1.0500	0.0000	1.5260	0.6584	0.00	0.00
2	1.0000	-2.6944	0.3000	-0.6512	0	0
3	0.9796	-6.2114	0	0	0.45	0.20
4	0.9776	-6.9232	0	0	0.80	0.30
5	0.9922	-6.6963	0	0	0.50	0.25

Using CIGRE's load model (iii), the configuration of the load is R parallel with X_L in series with X_s . Hence, the load in node 3, 4 and 5 can be calculated using the formula of

$$R = \frac{VLL^2}{P3\phi}, X_L(h) = j \frac{hR}{6.7(\frac{Q3\phi}{P3\phi} - 0.74)} \text{ and } X_s(h) = j0.073h \text{ while the capacitor bank can be}$$

calculated using the formula, $X_c(h) = -j \frac{VLL^2}{hQ3\phi}$. The calculated value for the load in node 3, 4 and 5 can be summarized as in table 4.

TABLE 4. Load impedance at node 3, 4 and 5 based on CIGRE's load model (iii)

Node	Load impedance, $Z_L = \frac{RX_L}{R+X_L} + X_s$	Capacitor bank, X_c
3	0.1711-jh0.3313	0
4	0.4333-jh0.7023	$-j \frac{3.1857}{h}$
5	0.5491-jh0.7391	0

The sample code for this test system can be viewed in the Appendix section. The results once the code is run composed of both frequency scan analysis and harmonic resonance mode analysis impedance vs frequency graph as shown in figure 6 and figure 7, respectively.

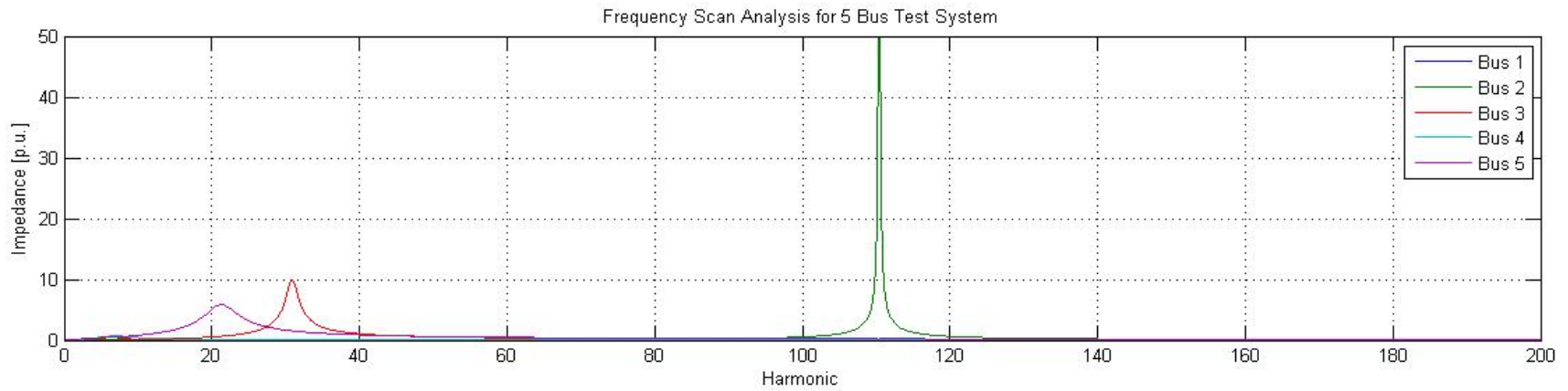


FIGURE 6. Frequency Scan Analysis Results of the Five Bust Test System

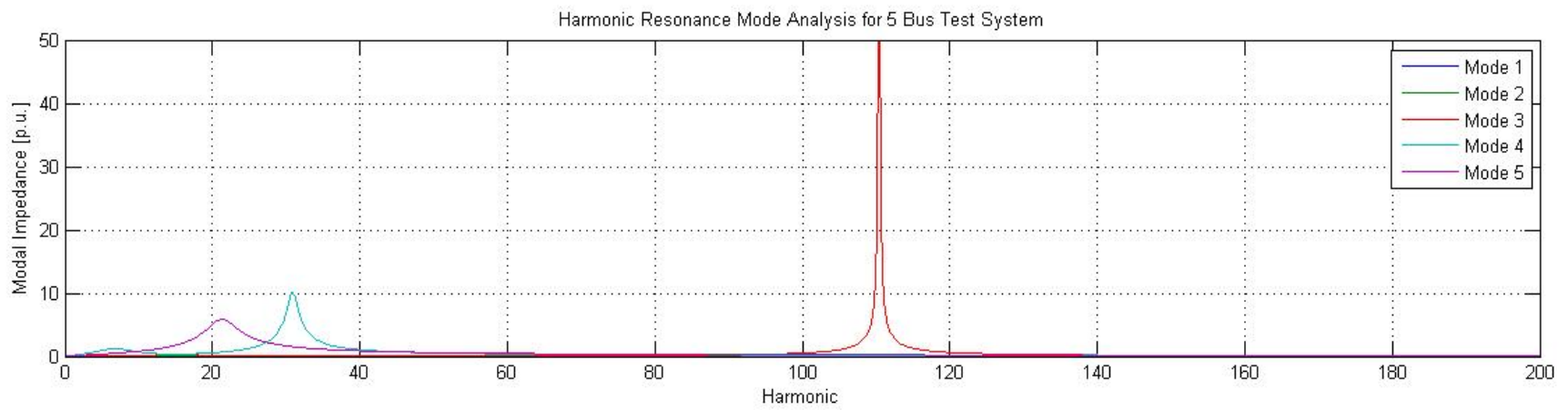


FIGURE 7. Modal Impedances of the Five Bust Test System

From figure 6, it can be observed that there are resonances created at bus 2, 3 and 5. The result is identical to the result of the harmonic resonance mode analysis technique in figure 7, which gives a high resonance at similar frequency with similar amplitude. As can be seen in the graph from harmonic resonance mode analysis, three modes are subjected to have high resonances which are mode 3, 4 and 5. A further analysis based on admittance matrix decomposition method to produce the eigenvalue and eigenvectors is conducted to further analysed the situation which can relate the results between these two methods if there are significance or relationship between the results. Table 5 shows the critical eigenvalue, critical eigenvectors and the participation factors for the three modes (mode 3, mode 4 and mode 5).

TABLE 5. Modal Analysis Results of the Five Bus Test System

Resonant frequency (p.u.)		21.3 (Mode 5)	30.9 (Mode 4)	110.4 (Mode 3)
Critical eigenvalue (D)		0.17/9.0667	0.1362/43.41	0.00282/-69.26
Right eigenvector (R)	Bus 1	R51=1.48x10 ⁻⁶ /-169.26	R41=4.2417x10 ⁻⁴ / <u>0.62367</u>	R31=0.00178/0.173
	Bus 2	R52=7.99x10 ⁻³ /0.987	R42=0.005237/0.6662	R32=0.9998/-0.0002
	Bus 3	R53=0.0355/-178.13	R43=0.9936/-0.025	R33=0.00889/-179.75
	Bus 4	R54=0.0262/-178.41	R44=0.1111/-179.04	R34=0.00117/-179.83
	Bus 5	R55=0.9989/-7.05x10 ⁻³	R45=0.0215/0.8792	R35=0.0178/-179.73
Left eigenvector (L)	Bus 1	L15=1.49x10 ⁻⁶ /-169.25	L14=4.24167x10 ⁻⁴ / <u>0.6489</u>	L13=0.00178/0.173
	Bus 2	L25=0.008/0.994	L24=0.005327/0.6914	L23=0.9998/0
	Bus 3	L35=0.0355/-178.12	L34=0.9936/0	L33=0.00889/-179.75
	Bus 4	L45=0.0262/-178.41	L44=0.1111/-179.02	L43=0.00117/-179.83
	Bus 5	L55=0.9989/0	L54=0.0215/0.9044	L53=0.0178/-179.73
Participation factor (RxL in magnitude)	Bus 1	PF15=2.212x10 ⁻¹²	PF14=1.799x10 ⁻⁷	PF13=3.1684x10 ⁻⁶
	Bus 2	PF25=6.241x10 ⁻⁵	PF24=2.8377x10 ⁻⁵	PF23=0.9996
	Bus 3	PF35=1.2617x10 ⁻³	PF34=0.9872	PF33=7.9032x10 ⁻⁵
	Bus 4	PF45=6.8696x10 ⁻⁴	PF44=0.0123	PF43=1.3689x10 ⁻⁶
	Bus 5	PF55=0.99798	PF54=4.6225x10 ⁻⁴	PF53=3.1684x10 ⁻⁴

From the results obtained, mode 5 achieved a resonance at 21.3 p.u. The result reveals that the key participating bus for mode 5 is bus 5, which indicates why the plotting in both graphs correlates bus 5 and mode 5 at the frequency of 21.3 p.u. For mode 4, a resonance is achieved at 30.9 p.u. and the key participating bus is said to be bus 3.

This is proven by the correlation between the two graphs whereby at 30.9 p.u., both Bus 3 and mode 4 achieved a high resonance with almost similar amplitude. Same goes to mode 5, which produces a resonance at a later frequency at 110.4, which coincides with Bus 2. From all these results, it can prove that there are some relationship between the results obtained from the frequency scan analysis method and the harmonic resonance mode analysis method. Even though the results are not as discrete and obvious as the previous example in the three bus test system, more or less this proves that the harmonic resonance mode analysis do have its own way in providing the information of revealing the location to observe or excite harmonic resonance.

Other than that, from the results obtained, it also proves that in some cases, there might be some possibilities that there might be some similarities in terms of the value of the impedance and the modal impedance, like what is happening in this five bus test system.

4.3 Standard IEEE 14 bus test system

After successfully tested the three buses and five buses system, the author moved on to do the testing on the IEEE 14 bus test system. Using the components available in the PSAT library, the standard IEEE 14 buses are constructed as shown in figure 8. The harmonic sources are not yet included just to show the comparison with and without harmonic sources with their impacts on the network.

The network was constructed and simulated in PSAT to determine the load flow before harmonic solutions are being conducted. Table 6 shows the results of the load flow result of this standard IEEE 14 bus test system.

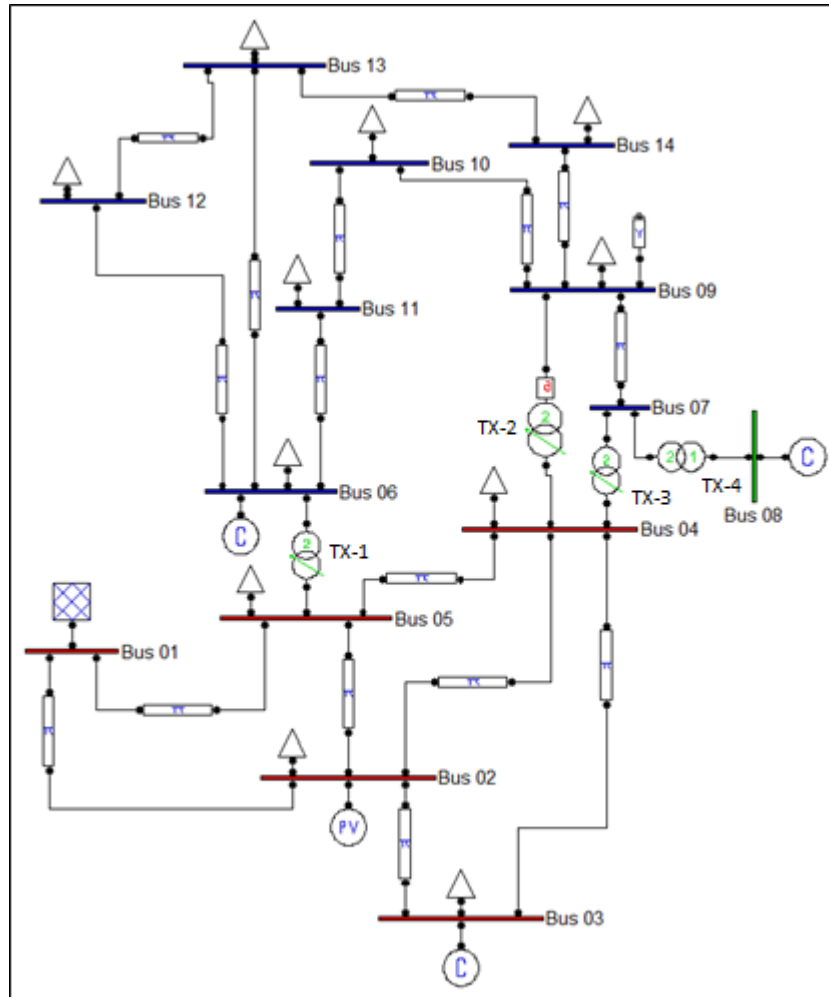


FIGURE 8. Standard IEEE 14 Bus Test System

TABLE 6. Load flow result for the standard IEEE 14 Bus Test system

Bus	Voltage [p.u.]	Angle [deg]	P gen [p.u.]	Q gen [p.u.]	P load [p.u.]	Q load [p.u.]
1	1.0600	0	2.3256	-0.15578	0	0
2	1.0450	-4.973	0.4	0.46087	0.217	0.127
3	1.0100	-12.686	0	0.25555	0.942	0.19
4	1.0150	-10.266	0	0	0.478	-0.04
5	1.0174	-8.8123	0	0	0.076	0.016
6	1.0700	-14.806	0	0.20731	0.112	0.075
7	1.0494	-14.213	0	0	0	0
8	1.0900	-14.213	0	0.25098	0	0
9	1.0321	-16.263	0	0	0.295	0.166
10	1.0311	-16.292	0	0	0.09	0.058
11	1.0466	-15.685	0	0	0.035	0.018
12	1.0535	-15.713	0	0	0.061	0.016
13	1.0467	-15.846	0	0	0.135	0.058
14	1.0202	-17.084	0	0	0.149	0.05

Upon conducting the load flow, the bus voltages as well as both the active power and reactive power are used to conduct the harmonic resonance study. These values are essential to determine the load admittance of the network which will determine the overall admittance matrix of the network. The formula to determine the admittance of the load will be based on CIGRE's load model (iii). As what have been implemented on the three and five bus test system, the same method is implemented on this standard IEEE 14 bus test system to evaluate the harmonic resonance in the network, which is through the implementation of the frequency scan analysis and the harmonic resonance mode analysis technique. The MATLAB code for this IEEE 14bus test system can be viewed in Appendix section. Figure 9 and figure 10 shows the results of the frequency scan analysis technique and the harmonic resonance mode analysis technique, respectively.

Based on figure 9 and figure 10, it can be seen that there are differences between the frequency scan analysis method and the harmonic analysis method like what have been mentioned in previous test system. The modes in figure 10 can be further analysed to determine the eigenvalue, eigenvector and also the participation factor. As can be seen on figure 10, the resonance occurs with three occasions in mode 4 which is at 20.0, 27.6 and 35.7 p.u. Other resonance occurs in mode 3 at 26.3 p.u. and in mode 2 at 36.7 p.u. Table 7 shows the critical eigenvalue and eigenvector as well as the participation factor for the modes involved.

As what can be seen in figure 9 at 20.0 p.u., there are multiple resonance occurring at that particular frequency. Through the calculation of the participation factor, it can be seen that in figure 10 that the resonance at 20.0 p.u. in mode 4 is caused mainly by bus 4. Mode 4 also indicates that some resonances are occurring at 27.6 and 35.7 p.u. Through the participation factor, the key participating bus involved at 27.6 p.u. is bus 1 while at 35.7 p.u. the bus involved is bus 4. This means that bus 1 and bus 4 has the largest possibilities that the resonance can be excited the most. Hence, controlling these two buses can be crucial in determining the degree of resonance at these particular frequencies.

Similarly with mode 2 which has the largest participation factor at bus 4 while mode 3 has its key participating buses as bus 1. It can be seen that the degree of observability of resonance is high at both bus 4 and bus 1. By controlling the parameters at bus 4 and bus 1, the resonance can be further analysed and controlled.

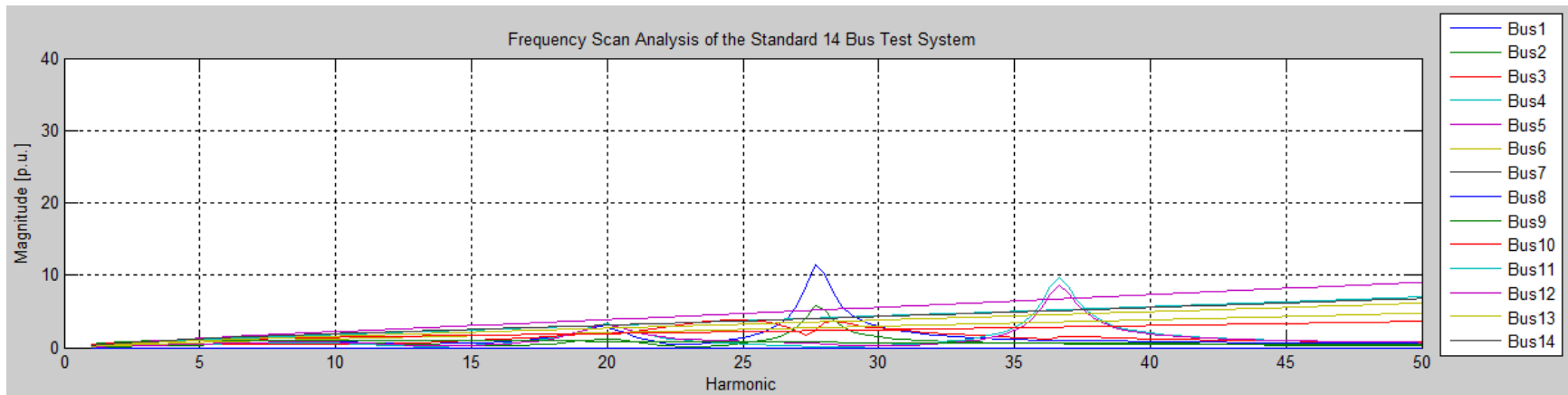


FIGURE 9. Frequency Scan Analysis of the Standard IEEE 14 Bus Test System

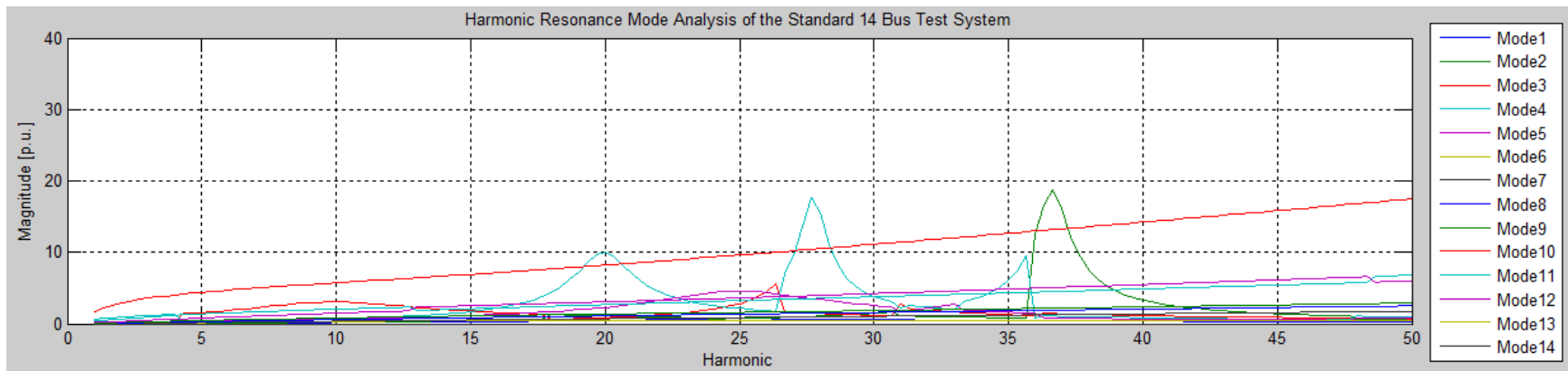


FIGURE 10. Harmonic Resonance Mode Analysis of the Standard IEEE 14 Bus Test System

TABLE 7. Modal Analysis Results for the Standard IEEE 14 Bus Test System

Resonant frequency (p.u.)		20.0 (Mode 4)	26.3 (Mode 3)	27.6 (Mode 4)	35.7 (Mode 4)	36.7 (Mode 2)
Critical eigenvalue (D)		0.0993/9.0356	0.1813/-72.20	0.05739/-13.09	0.10/-56.36	0.05375/10.83
Right eigenvector (R)	Bus 1	R41=0.5298/178.80	R31=0.7897/-7.904	R41=0.8273/-10.88	R41=0.082/-2.667	R21=0.081/-2.685
	Bus 2	R42=0.3438/173.69	R32=-0.6086/175.86	R42=0.5938/173.33	R42=0.0111/180.00	R22=0.01/180.00
	Bus 3	R43=0.2098/-28.46	R33=0.3368/23.9	R43=0.4111/26.06	R43=0.1556/-171.69	R23=0.160/-171.72
	Bus 4	R44=0.5724/1.902	R34=0.0116/114.36	R44=0.0172/136.17	R44=0.7208/2.067	R24=0.7191/2.008
	Bus 5	R45=0.5482/8.4228	R35=0.0805/-32.62	R45=0.0765/-51.84	R45=0.6731/179.51	R25=0.6738/179.51
	Bus 6 – Bus 14	R46-R414=0.0/0.0	R36-R314=0.0/0.0	R46-R414=0.0/0.0	R46-R414=0.0/0.0	R26-R214=0.0/0.0
Left eigenvector (L)	Bus 1	L14=0.5119/176.89	L13=0.7482 /0.000	L14=0.7514/0.173	L14=0.0816/-4.781	L12=0.0809/-4.675
	Bus 2	L24=0.3321/171.78	L23=0.5766/-176.23	L24=0.5393/-175.79	L24=0.011/177.91	L22=0.011/177.91
	Bus 3	L34=0.2028/-30.36	L33=0.3191/31.81	L34=0.3734/36.94	L34=0.1553/-173.75	L32=0.16/-173.72
	Bus 4	L44=0.5531/0.000	L43=0.0111/122.11	L44=0.0156/147.02	L44=0.7195/0.0	L42=0.7178/0.0
	Bus 5	L54=0.5297/6.525	L53=0.0762/-24.72	L54=0.0695/-40.97	L54=0.6719/177.45	L52=0.6726/177.5
	Bus 6 – Bus 14	L64-L144=0.0/0.0	L63-L143=0.0/0.0	L64-L144=0.0/0.0	L64-L144=0.0/0.0	L62-L142=0.0/0.0
Participation factor (R _x L in magnitude)	Bus 1	PF14=0.2712	PF13=0.5908	PF14=0.6216	PF14=6.69912x10 ⁻³	PF12=0.06553
	Bus 2	PF24=0.1142	PF23=0.3509	PF24=0.3202	PF24=1.221x10 ⁻⁴	PF22=1.1x10 ⁻³
	Bus 3	PF34=0.0425	PF33=0.1075	PF34=0.1535	PF34=0.0242	PF32=0.0256
	Bus 4	PF44=0.3166	PF43=1.2876x10 ⁻⁴	PF44=2.6832x10 ⁻⁴	PF44=0.5186	PF42=0.5161
	Bus 5	PF54=0.2904	PF53=6.1341x10 ⁻³	PF54=5.3168x10 ⁻³	PF54=0.4523	PF52=0.4532
	Bus 6 – Bus 14	PF64-PF144=0.00	PF63-PF143=0.00	PF64-PF144=0.00	PF64-PF144=0.00	PF62-PF142=0.00

4.4 Modified IEEE 14 bus test system

Next, the harmonic sources are included to show their impacts on the network. For the purpose of analyzing the frequency scan and harmonic resonance mode analysis technique, the load flow results and branch data are taken from [1] to ensure data reliability and the result was compared and analysed. Based on the information from [1], the MATLAB code was altered a bit whereby the code for harmonic filters is included to study their effects and significance. The results can be viewed as shown in figure 11 and figure 12.

As can be seen in figure 12, high resonance involving mode 2, mode 4 and mode 5 occurs as a result of the presence of harmonic sources which are HVDC and SVC. The HVDC is modelled as a two-six pulse converter while the SVC is modelled as a delta-connected TCR. [1] suggested that the impact of the component at bus 8 (SVC) on the network harmonic distortion is smaller compared to bus 3 (HVDC). Table 8 and table 9 shows the modal analysis result of the modified IEEE 14 bus test system while table 10 shows the summarization of table 8 and table 9.

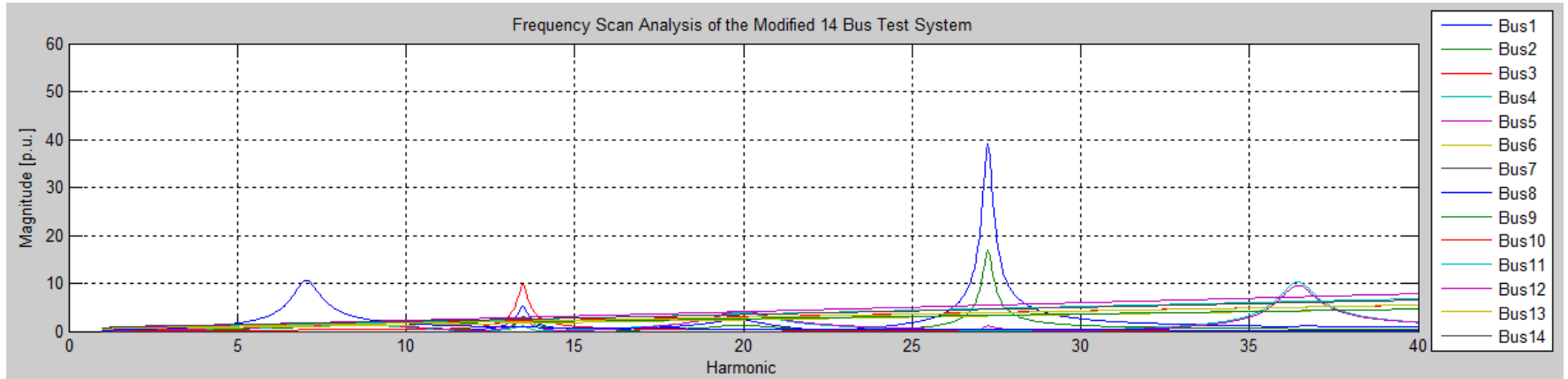


FIGURE 11. Frequency Scan Analysis for the Modified IEEE 14 Bus Test System

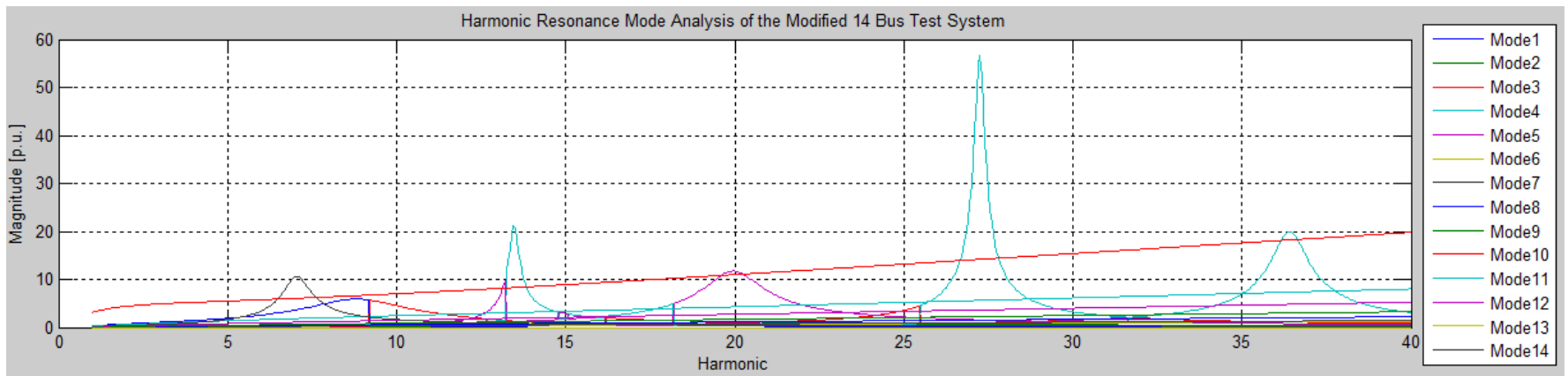


FIGURE 12. Harmonic Resonance Mode Analysis for the Modified IEEE 14 Bus Test System

TABLE 8. Modal Analysis Results for the Modified IEEE 14 Bus Test System

Resonant frequency (p.u.)	7.1 (Mode 14)	9.1 (Mode 1)	9.2 (Mode 3)	13.2 (Mode 5)	
Critical eigenvalue (D)	0.095/ <u>13.51</u>	0.1727/ <u>25.44</u>	0.175/ <u>29.09</u>	0.1018/ <u>-63.96</u>	
Right eigenvector (R)	Bus 1	R141=0.0/ <u>0.0</u>	R11=0.4789/ <u>3.844</u>	R31=0.4787/ <u>3.77</u>	R51=0.465/ <u>-176.6</u>
	Bus 2	R142=0.0/ <u>0.0</u>	R12=-0.4852/ <u>1.618</u>	R32=0.4859/ <u>1.568</u>	R52=0.3438/ <u>-176.43</u>
	Bus 3	R143=0.0/ <u>0.0</u>	R13=0.22/ <u>-0.702</u>	R33=0.224/ <u>-0.716</u>	R53=0.7284/ <u>-4.023</u>
	Bus 4	R144=0.0/ <u>0.0</u>	R14=0.4909/ <u>-10.16</u>	R34=0.4896/ <u>-10.15</u>	R54=0.197/ <u>168.26</u>
	Bus 5	R145=0.0/ <u>0.0</u>	R15=0.5303/ <u>-5.139</u>	R35=0.5289/ <u>-5.163</u>	R55=0.3416/ <u>174.74</u>
	Bus 6 – Bus 14	R146-R414=0.0/ <u>0.0</u> except R148=1.000/ <u>0.0</u>	R16-R114=0.0/ <u>0.0</u>	R36-R314=0.0/ <u>0.0</u>	R56-R514=0.0/ <u>0.0</u>
Left eigenvector (L)	Bus 1	L14=0.0/ <u>0.0</u>	L13=0.4706 / <u>8.986</u>	L13=0.4705/ <u>8.938</u>	L15=0.4603/ <u>-4.781</u>
	Bus 2	L24=0.0/ <u>0.0</u>	L23=0.4768/ <u>6.757</u>	L23=0.4777/ <u>6.732</u>	L25=0.3403/ <u>-172.42</u>
	Bus 3	L34=0.0/ <u>0.0</u>	L33=0.2164/ <u>4.425</u>	L33=0.2202/ <u>4.455</u>	L35=0.7210/ <u>0.0</u>
	Bus 4	L44=0.0/ <u>0.0</u>	L43=0.4824/ <u>-5.018</u>	L43=0.4812/ <u>-4.995</u>	L45=0.195/ <u>172.2</u>
	Bus 5	L54=0.0/ <u>0.0</u>	L53=0.5212/ <u>0.0</u>	L53=0.5199/ <u>0.0</u>	L55=0.3382/ <u>178.76</u>
	Bus 6 – Bus 14	L64-L144=0.0/ <u>0.0</u> except R148=1.000/ <u>0.0</u>	L63-L143=0.0/ <u>0.0</u>	L63-L143=0.0/ <u>0.0</u>	L65-L145=0.0/ <u>0.0</u>
Participation factor (RxL in magnitude)	Bus 1	PF114=0.0	PF11=0.2254	PF13=0.2252	PF15=0.214
	Bus 2	PF214=0.0	PF21=0.2313	PF23=0.2321	PF25=0.117
	Bus 3	PF314=0.0	PF31=0.0476	PF33=0.0493	PF35=0.525
	Bus 4	PF414=0.0	PF41=0.2368	PF43=0.2356	PF45=0.0384
	Bus 5	PF514=0.0	PF51=0.2763	PF53=0.2749	PF55=0.1155
	Bus 6 – Bus 14	PF614-PF1414=0.00 except PF814=1.000	PF61-PF141=0.00	PF63-PF143=0.00	PF65-PF145=0.00

TABLE 9. Modal Analysis Results for the Modified IEEE 14 Bus Test System (continued)

Resonant frequency (p.u.)		13.4 (Mode 4)	19.9 (Mode 5)	27.2 (Mode 4)	36.4 (Mode 4)
Critical eigenvalue (D)		0.0517/ <u>-26.12</u>	0.0853/ <u>0.0</u>	0.018/ <u>-14.26</u>	0.05/ <u>0.573</u>
Right eigenvector (R)	Bus 1	R41=0.4784/ <u>-176.92</u>	R51=0.4483/ <u>-178.58</u>	R41=0.8285/ <u>-0.325</u>	R41=0.0888/ <u>-1.742</u>
	Bus 2	R42=0.3686/ <u>-176.95</u>	R52=0.3247/ <u>177.49</u>	R42=-0.5461/ <u>-179.77</u>	R42=0.02/ <u>-176.28</u>
	Bus 3	R43=0.6897/ <u>-4.515</u>	R53=0.0274/ <u>-171.39</u>	R43=0.0175/ <u>0.3274</u>	R43=0.0124/ <u>-177.23</u>
	Bus 4	R44=0.2221/ <u>168.57</u>	R54=0.5869/ <u>3.155</u>	R44=0.0116/ <u>114.36</u>	R44=0.7194/ <u>2.27</u>
	Bus 5	R45=0.3635/ <u>174.60</u>	R55=0.6014/ <u>7.683</u>	R45=0.1221/ <u>-0.375</u>	R45=0.6898/ <u>179.94</u>
	Bus 6 – Bus 14	R46-R414=0.0/ <u>0.0</u>	R56-R514=0.0/ <u>0.0</u>	R46-R414=0.0/ <u>0.0</u>	R46-R414=0.0/ <u>0.0</u>
Left eigenvector (L)	Bus 1	L14=0.4731/ <u>-172.41</u>	L15=0.4454/ <u>173.74</u>	L14=0.8284/ <u>0.000</u>	L14=0.0887/ <u>-4.007</u>
	Bus 2	L24=0.3647/ <u>-172.44</u>	L25=0.3226/ <u>169.80</u>	L24=0.546/ <u>-179.44</u>	L24=0.02/ <u>-178.57</u>
	Bus 3	L34=0.6823/ <u>0.0</u>	L35=0.0272/ <u>-179.16</u>	L34=0.0175/ <u>0.655</u>	L34=0.0124/ <u>-179.54</u>
	Bus 4	L44=0.2197/ <u>173.10</u>	L45=0.5831/ <u>-4.525</u>	L44=0.0185/ <u>169.42</u>	L44=0.7187/ <u>0.0</u>
	Bus 5	L54=0.3595/ <u>179.12</u>	L55=0.5974/ <u>0.0</u>	L54=0.122/ <u>-0.047</u>	L54=0.6893/ <u>177.68</u>
	Bus 6 – Bus 14	L64-L144=0.0/ <u>0.0</u>	L65-L145=0.0/ <u>0.0</u>	L64-L144=0.0/ <u>0.0</u>	L64-L144=0.0/ <u>0.0</u>
Participation factor (R _x L in magnitude)	Bus 1	PF14=0.2263	PF15=0.1997	PF14=0.6863	PF14=7.8766x10 ⁻³
	Bus 2	PF24=0.1344	PF25=0.1047	PF24=0.2982	PF24=4.0x10 ⁻⁴
	Bus 3	PF34=0.4706	PF35=7.4528x10 ⁻⁴	PF34=3.0625x10 ⁻⁴	PF34=1.5376x10 ⁻⁴
	Bus 4	PF44=0.0488	PF45=0.3422	PF44=2.146x10 ⁻⁴	PF44=0.5170
	Bus 5	PF54=0.1307	PF55=0.3593	PF54=14.89x10 ⁻³	PF54=0.4755
	Bus 6 – Bus 14	PF64-PF144=0.00	PF65-PF145=0.00	PF64-PF144=0.00	PF64-PF144=0.00

TABLE 10. Summary of the modal results on the modified IEEE 14 bus network

Modal Resonance Frequency Order h (pu)	Modes involved	Critical Eigenvalue Magnitude	Largest PFs	Most Participating Bus
7.1	14	0.0950	1.0000	8
9.1	1	0.1727	0.2750	5
9.3	3	0.1789	0.2724	5
13.2	5	0.1018	0.5238	3
13.4	4	0.0517	0.4691	3
19.9	5	0.0853	0.3561	5
27.2	4	0.0182	0.6863	1
36.4	4	0.0500	0.5166	4

It can be seen that bus 5 affects the resonance largely at both frequency of 9.1, 9.3 and 19.9 p.u. while bus 3 affects mainly at a frequency order of 13.2 and 13.4 p.u. Bus 8 affects at a lower order of 7.1, while bus 1 and bus 4 affects at a frequency of 27.2 and 36.4, respectively. Due to the reason of investigating the suggestion made in [1], the author focus on the discussing this issue on bus 3 and bus 8 only.

From table 10 and figure 12, it can be concluded that the resonance at bus 8 affects at a lower magnitude compared to the HVDC at bus 3. As stated previously, smaller eigenvalue indicates a larger value of modal impedance. This theory is proven through the results presented in both table 10 and figures 12 which tells why the modal impedance at one of the mode involving bus 3 as its key participating bus (mode 4) has a higher modal impedance compared to the mode 14 which has bus 8 as its key participating bus. Injecting modal 5 current will cause a large modal 5 voltage to be produced. Hence, the impact on bus 3 voltages will be much higher compared to bus 8.

The high value of PF at bus 8 indicates that the probability of observing and exciting the resonance is very high at bus 8. This might be due to the effects of HVDC and the installation of harmonic filters at that particular bus, at which four harmonic filters are installed in the order of 2, 5, 7 and 11. Bus 3 also has a high value of PF but not as high as the PF at bus 8. Hence, observing the components and other conditions through these buses can be critical in controlling the resonance produced.

4.5 UTP new academic building network

Upon finishing the test on both the standard and modified IEEE 14 Buses test system, the author proceeds on gathering the data and information regarding the UTP distribution network. The process of finding and searching for the network data has begun. The process was not that easy as expected.

However, upon setting up a meeting with one of the assistant engineer who owns the UTP network data, the process of understanding the single line diagram became a bit easier. With some visits conducted at the low voltage (LV) room as well as the underground room for the Block 23, the author managed to grab the idea of how the network cables went through from the gas district cooling (GDC) building to the entire academic building.

The entire UTP network is basically supported by two 4.2MW Taurus 60 gas turbine generators, which combines to give a total supply of 8.4MW. These two generators are basically situated at the GDC, whereby it will be connected to the main intake substation (MIS) switchgear board. From there, the 11kV voltage will run through the high voltage (HV) board before being stepped down through an 11kV/413V step down transformer to be supplied to the LV board and distributed throughout the academic blocks.

For the author to conduct the frequency scan analysis as well as the harmonic resonance mode analysis technique, the load flow study for the UTP new academic building need to be constructed. The impedance and admittance base values for both HV and LV side are calculated and assembled in table 11. Figure 13 shows the simplified single diagram that has been rebuilt using the MATLAB. Upon constructed the single line diagram in MATLAB, the load flow is performed and table 12 shows the load flow results for the UTP new academic building network.

TABLE 11. Cable parameters for UTP new academic building network

Cable	Length, l (km)	Resistance/km (Ω /km)	Reactance/km (Ω /km)	Capacitance/km (μ F/km)	Resistance, [p.u.]	Reactance [p.u.]	Susceptance [p.u.]
1	0.864	0.0984	0.089	0.48	0.007026	0.006325	0.001580
2	0.860	0.0984	0.089	0.48	0.006994	0.006325	0.001570
3	0.550	0.0984	0.089	0.48	0.004470	0.004045	0.001000
4	0.546	0.0984	0.089	0.48	0.004440	0.004016	0.000996
5	0.014	0.128	0.092	0.43	0.000148	0.000106	0.000106
6	0.339	0.128	0.092	0.43	0.003586	0.002580	0.002580
7	0.362	0.128	0.092	0.43	0.003829	0.002750	0.002750
8	0.673	0.128	0.092	0.43	0.007120	0.005120	0.005120
9	0.012	0.128	0.092	0.43	0.000126	0.000091	9.124x10-5
10	0.688	0.128	0.092	0.43	0.007278	0.005230	0.005230
11	0.983	0.128	0.092	0.43	0.009869	0.007093	0.001607
12	0.341	0.128	0.092	0.43	0.003607	0.002593	0.002593
13	0.014	0.128	0.092	0.43	0.000148	0.000106	2.289x10-5
14	0.007	8.48u Ω /m	3.77u Ω /m	0	0.003165	4.94x10-7	0
15	0.013	12.5u Ω /m	4.0u Ω /m	0	0.008667	9.75x10-7	0
16	0.013	12.5u Ω /m	4.0u Ω /m	0	0.008667	9.75x10-7	0
17	0.010	20.3u Ω /m	9.3u Ω /m	0	0.010826	1.74x10-6	0
18	0.055	0.0793	0.0920	0	0.232600	9.48x10-5	0
19	0.013	12.5u Ω /m	4.0u Ω /m	0	0.008667	9.75x10-7	0
20	0.010	20.3u Ω /m	9.3u Ω /m	0	0.010826	1.74x10-6	0
21	0.007	8.48u Ω /m	3.77u Ω /m	0	0.003166	4.95x10-7	0
22	0.017	12.5u Ω /m	4.0u Ω /m	0	0.011333	1.27x10-6	0

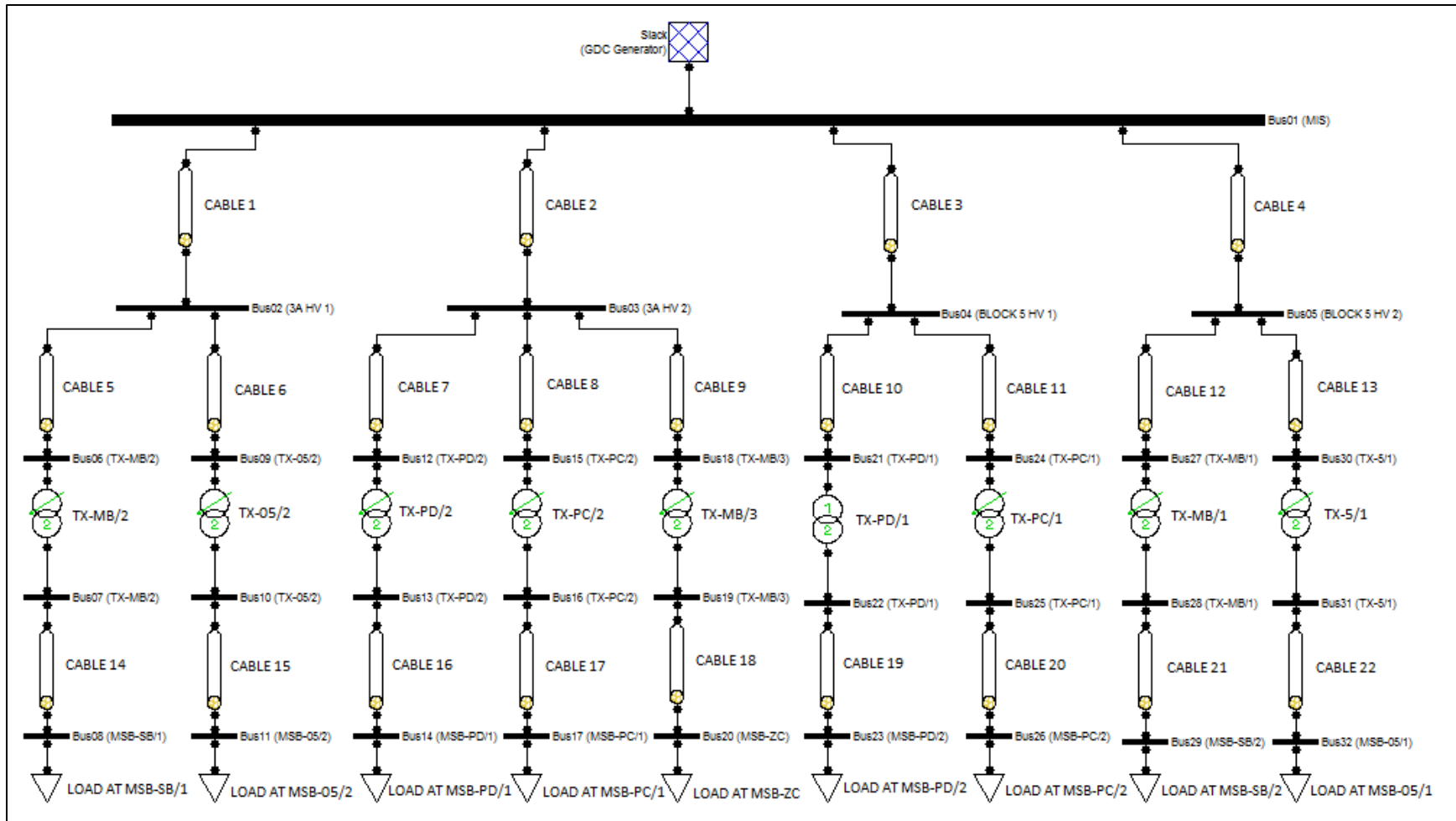


FIGURE 13. Simplified single line diagram for UTP new academic building network

TABLE 12. Load flow results for UTP new academic building network

Bus	Voltage [p.u.]	Angle [deg]	P gen [p.u.]	Q gen [p.u.]	P load [p.u.]	Q load [p.u.]
1	1.000	0	0.80166	0.35046	0	0
2	0.99832	-0.02516	0	0	0	0
3	0.99864	-0.0084	0	0	0	0
4	0.99885	-0.0189	0	0	0	0
5	1.001	-0.05548	0	0	0	0
6	0.9983	-0.02531	0	0	0	0
7	0.99521	-0.36095	0	0	0	0
8	0.9949	-0.02808	0	0	0.0097	0.051
9	0.998	-0.25634	0	0	0	0
10	0.996	-0.00814	0	0	0	0
11	0.99542	-0.25039	0	0	0.0066	0.033
12	0.99823	-0.00713	0	0	0	0
13	0.99515	-0.11527	0	0	0	0
14	0.99453	-0.00842	0	0	0.007	0.051
15	0.99829	-0.06705	0	0	0	0
16	0.99675	-0.03292	0	0	0	0
17	0.99641	-0.44519	0	0	0.00313	0.0255
18	0.99864	-0.02277	0	0	0	0
19	0.99809	-0.23032	0	0	0	0
20	0.99411	-0.39095	0	0	0.0017	0.009
21	0.99771	-1.2726	0	0	0	0
22	0.99461	-0.05567	0	0	0	0
23	0.99357	-0.35306	0	0	0.0119	0.051
24	0.99801	-0.42121	0	0	0	0
25	0.99583	-0.02412	0	0	0	0
26	0.99518	-0.23185	0	0	0.006	0.036
27	1.0081	-0.20932	0	0	0	0
28	1.005	-0.57328	0	0	0	0
29	1.0042	-1.4359	0	0	0.0254	0.051
30	1.001	-0.24032	0	0	0	0
31	0.99892	-0.53632	0	0	0	0
32	0.99794	-0.51352	0	0	0.0086	0.0035

The base power used for this network is 10MVA while the loads are assumed to be operating at 30% of the critical load (CL) based on the power rating in the single line diagram provided. The configuration used for the transmission line is the nominal-pi model. From the load flow results in table 12, the voltage buses, active and reactive power are used for the simulation of harmonic resonance through frequency scan analysis and harmonic resonance mode analysis technique. The results can be viewed in figure 14 and figure 15.

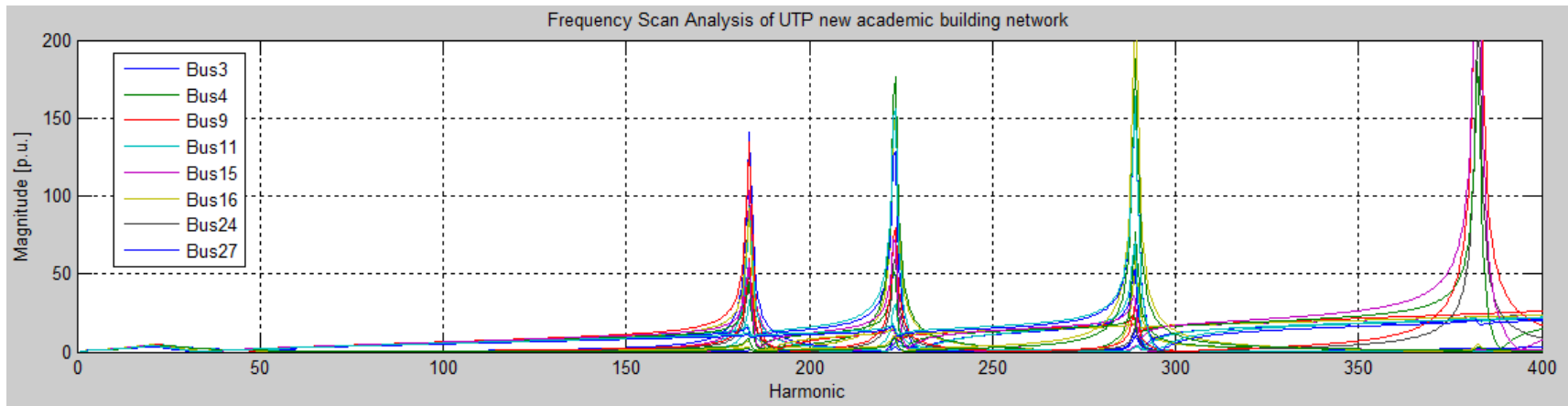


FIGURE 14. Frequency Scan Analysis of UTP new academic building network

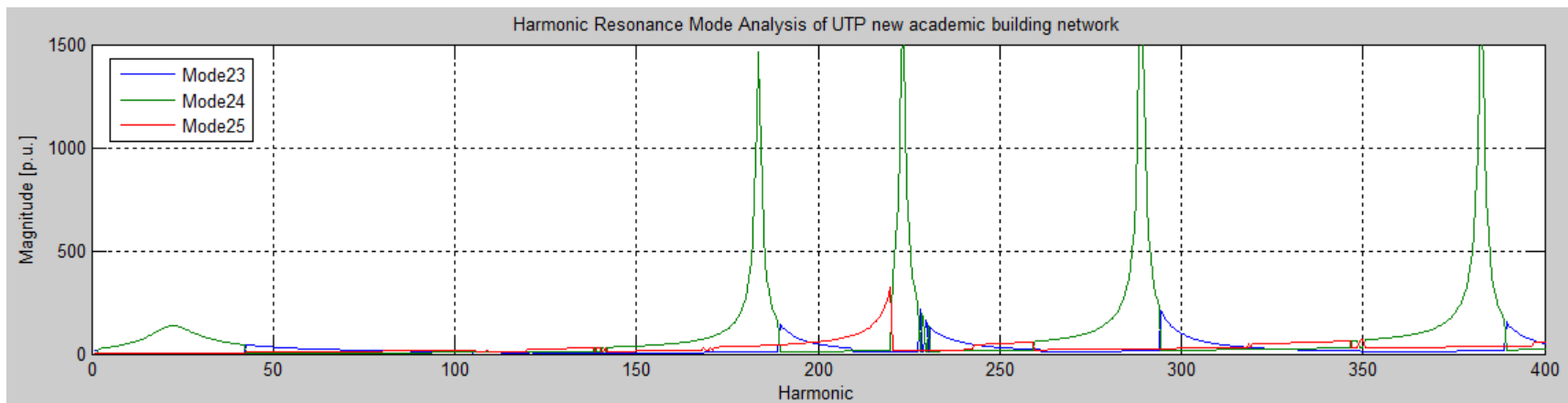


FIGURE 15. Harmonic Resonance Mode Analysis for UTP new academic building network

Due to time constraint, little analysis could be done for this test system. The author only did some part of the participation factor to understand the correlation and significant of the harmonic resonance mode analysis technique compared to the frequency scan analysis technique. From figure 14, it can be seen that there are resonances at frequency 21, 183.5, 223.5, 289 and 382 p.u. From the figure itself, it is almost impossible to figure out which buses actually took part in causing the resonance in the network. As there are multiple plots and peaks of resonance, this can be difficult to identify the resonance at those particular frequencies. Hence, further analysis need to be made which utilizes the modal-based analysis technique.

Based on figure 15, there are three modes that can be observed which are mode 23, mode 24 and mode 25. The author included these three modes only as the other modes show less significant to the system compared to these three modes. It can be seen that there are multiple peaks produced by these three modes. Based on the observation, mode 23 produces resonances at frequencies of 189.5 and 228p.u. Mode 24 has the highest number of peaks at which the resonances occur at a frequency of 22.5, 183.5, 223.5, 289 and 382.5 p.u. while mode 25 produces resonance at 220 p.u. frequency. These modes can be further analysed to determine their participation factors which can determine the key participating buses that actually influence the resonance in the network. Table 13 and table 14 shows the resonance mode information on UTP new academic building network. Table 15 shows the summary of the modal analysis for this network.

TABLE 13. Resonance mode information on UTP new academic building network

Resonant frequency (p.u.)	22.5 (Mode 24)	183.5 (Mode 24)	189.5 (Mode 23)	220 (Mode 25)	
Critical eigenvalue (D)	0.00729/ <u>26.91</u>	6.831x10-4/ <u>-5.58</u>	0.00683/ <u>84.12</u>	0.00670/ <u>-26.56</u>	
Participation factor (RxL in magnitude)	Bus 1	PF124=0.03356	PF124=8.2944x10-4	PF123=8.6436x10-4	PF123=0.001466
	Bus 2	PF224=0.03327	PF224=4.6512x10-3	PF223=4.5832x10-3	PF223=0.086970
	Bus 3	PF324=0.03386	PF324=0.06325	PF323=0.07474	PF323=0.002883
	Bus 4	PF424=0.03371	PF424=0.02298	PF423=0.02759	PF423=0.017875
	Bus 5	PF524=0.03287	PF524=0.00160	PF523=0.00161	PF523=0.004489
	Bus 6	PF624=0.03327	PF624=4.6512x10-3	PF623=4.5833x10-3	PF623=0.087025
	Bus 7	PF724=0.02907	PF724=3.9942x10-3	PF723=3.0030x10-3	PF723=0.086981
	Bus 8	PF824=0.02907	PF824=3.9942x10-3	PF823=3.0030x10-3	PF823=0.086981
	Bus 9	PF924=0.03316	PF924=5.1122x10-3	PF923=4.9843x10-3	PF923=0.100996
	Bus 10	PF1024=0.03010	PF1024=4.6104x10-3	PF1023=3.410x10-3	PF1023=0.103603
	Bus 11	PF1124=0.03007	PF1124=4.6104x10-3	PF1123=3.410x10-3	PF1123=0.106210
	Bus 12	PF1224=0.03375	PF1224=0.0704	PF1223=0.08225	PF1223=0.003422
	Bus 13	PF1324=0.03052	PF1324=0.0631	PF1323=0.05598	PF1323=0.003576
	Bus 14	PF1424=0.03052	PF1424=0.0631	PF1423=0.05598	PF1423=0.003576
	Bus 15	PF1524=0.03389	PF1524=0.09585	PF1523=0.11189	PF1523=0.005580
	Bus 16	PF1624=0.03208	PF1624=0.09132	PF1623=0.08031	PF1623=0.006225
	Bus 17	PF1724=0.03208	PF1724=0.09132	PF1723=0.08031	PF1723=0.006225
	Bus 18	PF1824=0.03386	PF1824=0.06325	PF1823=0.07469	PF1823=0.002883
	Bus 19	PF1924=0.03258	PF1924=0.06170	PF1923=0.05471	PF1923=0.003306
	Bus 20	PF2024=0.03258	PF2024=0.06170	PF2023=0.05471	PF2023=0.003306
	Bus 21	PF2124=0.03342	PF2124=0.03508	PF2123=0.04169	PF2123=0.035118
	Bus 22	PF2224=0.02843	PF2224=0.02913	PF2223=0.02657	PF2223=0.033782
	Bus 23	PF2324=0.02839	PF2324=0.02913	PF2323=0.02657	PF2323=0.033782
	Bus 24	PF2424=0.03359	PF2424=0.04104	PF2423=0.04840	PF2423=0.046182
	Bus 25	PF2524=0.03069	PF2524=0.03736	PF2523=0.03337	PF2523=0.03337
	Bus 26	PF2624=0.03069	PF2624=0.03736	PF2623=0.03337	PF2623=0.03337
	Bus 27	PF2724=0.03247	PF2724=1.7389x10-3	PF2723=1.739x10-3	PF2723=1.739x10-3
	Bus 28	PF2824=0.02347	PF2824=1.1972x10-3	PF2823=9.425x10-3	PF2823=9.425x10-3
	Bus 29	PF2924=0.02347	PF2924=1.1972x10-3	PF2923=9.425x10-3	PF2923=9.425x10-3
	Bus 30	PF3024=0.03287	PF3024=0.0016	PF3023=0.00161	PF3023=0.00161
	Bus 31	PF3124=0.02876	PF3124=1.3988x10-3	PF3123=1.076x10-3	PF3123=1.076x10-3
	Bus 32	PF3224=0.02910	PF3224=1.3988x10-3	PF3223=1.076x10-3	PF3223=1.076x10-3

TABLE 14. Resonance mode information on UTP new academic building network (cont.)

Resonant frequency (p.u.)	223.5 (Mode 24)	228 (Mode 23)	289 (Mode 24)	382.5 (Mode 24)	
Critical eigenvalue (D)	$6.257 \times 10^{-4} / 13.8$	$0.00463 / 82.57$	$5.2388 \times 10^{-4} / 0.42$	$5.928 \times 10^{-4} / -6.29$	
Participation factor (RxL in magnitude)	Bus 1	PF124=0.03356	PF124=0.002106	PF123=0.00714	PF124=0.00204
	Bus 2	PF224=0.03327	PF224=0.107912	PF223=0.03150	PF224=0.00739
	Bus 3	PF324=0.03386	PF324=0.004108	PF323=0.00149	PF324=0.00289
	Bus 4	PF424=0.03371	PF424=0.021345	PF423=0.00224	PF424=0.00282
	Bus 5	PF524=0.03287	PF524=0.006177	PF523=0.09828	PF524=0.00183
	Bus 6	PF624=0.03327	PF624=0.107846	PF623=0.03150	PF624=7.396x10-5
	Bus 7	PF724=0.02907	PF724=0.074201	PF723=0.02699	PF724=7.396x10-5
	Bus 8	PF824=0.02907	PF824=0.074201	PF823=0.02699	PF824=6.4x10-5
	Bus 9	PF924=0.03316	PF924=0.123482	PF923=0.04044	PF924=1.166x10-4
	Bus 10	PF1024=0.03010	PF1024=0.088685	PF1023=0.03633	PF1024=1.06x10-4
	Bus 11	PF1124=0.03007	PF1124=0.088685	PF1123=0.03633	PF1124=1.06x10-4
	Bus 12	PF1224=0.03375	PF1224=0.004788	PF1223=0.00199	PF1224=4.84x10-4
	Bus 13	PF1324=0.03052	PF1324=0.003422	PF1323=0.00178	PF1324=4.41x10-6
	Bus 14	PF1424=0.03052	PF1424=0.003422	PF1423=0.00178	PF1424=4.41x10-6
	Bus 15	PF1524=0.03389	PF1524=0.007832	PF1523=0.00529	PF1524=9.02x10-5
	Bus 16	PF1624=0.03208	PF1624=0.005913	PF1623=0.00502	PF1624=8.649x10-5
	Bus 17	PF1724=0.03208	PF1724=0.005913	PF1723=0.00502	PF1724=8.649x10-5
	Bus 18	PF1824=0.03386	PF1824=0.004096	PF1823=0.00149	PF1824=2.89x10-6
	Bus 19	PF1924=0.03258	PF1924=0.003158	PF1923=0.00146	PF1924=2.89x10-6
	Bus 20	PF2024=0.03258	PF2024=0.003158	PF2023=0.00146	PF2024=2.89x10-6
	Bus 21	PF2124=0.03342	PF2124=0.041697	PF2123=0.00840	PF2124=0.13075
	Bus 22	PF2224=0.02843	PF2224=0.027822	PF2223=0.00695	PF2224=0.10877
	Bus 23	PF2324=0.02839	PF2324=0.027822	PF2323=0.00695	PF2324=0.10877
	Bus 24	PF2424=0.03359	PF2424=0.054103	PF2423=0.01656	PF2424=0.22448
	Bus 25	PF2524=0.03069	PF2524=0.039164	PF2523=0.01503	PF2524=0.20457
	Bus 26	PF2624=0.03069	PF2624=0.039164	PF2623=0.01503	PF2624=0.20457
	Bus 27	PF2724=0.03247	PF2724=0.007344	PF2723=0.12503	PF2724=0.00289
	Bus 28	PF2824=0.02347	PF2824=0.003956	PF2823=0.08585	PF2824=0.00199
	Bus 29	PF2924=0.02347	PF2924=0.003956	PF2923=0.08585	PF2924=0.00199
	Bus 30	PF3024=0.03287	PF3024=0.006084	PF3023=0.09834	PF3024=0.00183
	Bus 31	PF3124=0.02876	PF3124=0.004316	PF3123=0.08567	PF3124=0.00160
	Bus 32	PF3224=0.02910	PF3224=0.004316	PF3223=0.08567	PF3224=0.00160

TABLE 15. Summary of the modal results on the UTP new academic building network

Modal Resonance Frequency Order h (pu)	Modes involved	Critical Eigenvalue Magnitude	Largest PFs	Most Participating Bus
22.5	24	0.00729	0.0339	15
183.5	24	6.831×10^{-4}	0.0959	15
189.5	23	0.00684	0.1119	15
220	25	0.00670	0.1062	11
223.5	24	6.257×10^{-4}	0.0339	15
228	23	0.00463	0.1235	9
289	24	5.238×10^{-4}	0.1250	27
382.5	24	5.928×10^{-4}	0.2245	24

From table 15, it can be observed through the participation factor that bus 15 has the most potential to observe and excite resonance in the network at a frequency of 22.5, 183.5, 189.5 as well as 223.5 p.u. Through frequency scan analysis method, there are several number of buses which contributes to resonance at that particular frequencies. Through the computation of modal based technique, the highest observability and excitability of resonance can be found at bus 15 at which analysis and further precaution steps can be taken through monitoring the resonance at this particular bus.

Other resonances involve bus 9, 11, 24 and 27 at their respective resonant frequencies. From this information, it can be acknowledged that observing the resonance through these buses can be the key to mitigate further resonance implications. This is due to the fact that these buses also have the highest excitability to produce the highest resonance in this network. Hence, by observing the conditions at this bus, the critical resonance that is occurring through the UTP new academic building can be observed and further analysed. Consideration on reducing the effects of harmonic resonance at that particular frequency by placing harmonic filters can be a good idea but again the planning need to be precise as misplacing the filters can affect other components in the network.

CHAPTER 5

CONCLUSION AND RECOMMENDATION

5.1 Conclusion

The aim of the project is to implement the harmonic resonance mode analysis technique on several test systems as well as to model and simulate UTP new academic building using MATLAB software utilizing real parameters and data. This has been achieved through the results presented in this report.

From the results obtained, it can be verified that:

- Resonance actually occurs through specific mode whereby the mode can be determined through the smallest/ critical eigenvalue of the admittance matrix of the network.
- It is difficult to know which bus actually can be excited the most when being injected with harmonic current. Hence, by examining and identifying the key participating bus through the participation factor can help to solve this problem.
- The bus with the largest participation factor has the highest observability and excitability of resonance. This can be calculated through the left and right eigenvectors whereby the product gives the center occurrence of resonance.

5.2 Recommendation

From this study, there are a few recommendations to improve the efficiency of results in identifying resonance in a particular network.

1. Conduct a proper harmonic resonance analysis on UTP distribution network.

Through this implementation, the results can be made as a standard guideline for future use. For UTP network, there is less study made on harmonics as well as resonance. This is due to the fact that the big neutral cable on the generators side enables the harmonics to be grounded easily. Hence, no big issue regarding harmonics can be observed in UTP. However, for future use and emergency case, a proper harmonic resonance analysis should be conducted.

2. Conduct frequency scan analysis first to identify harmful resonance frequencies.

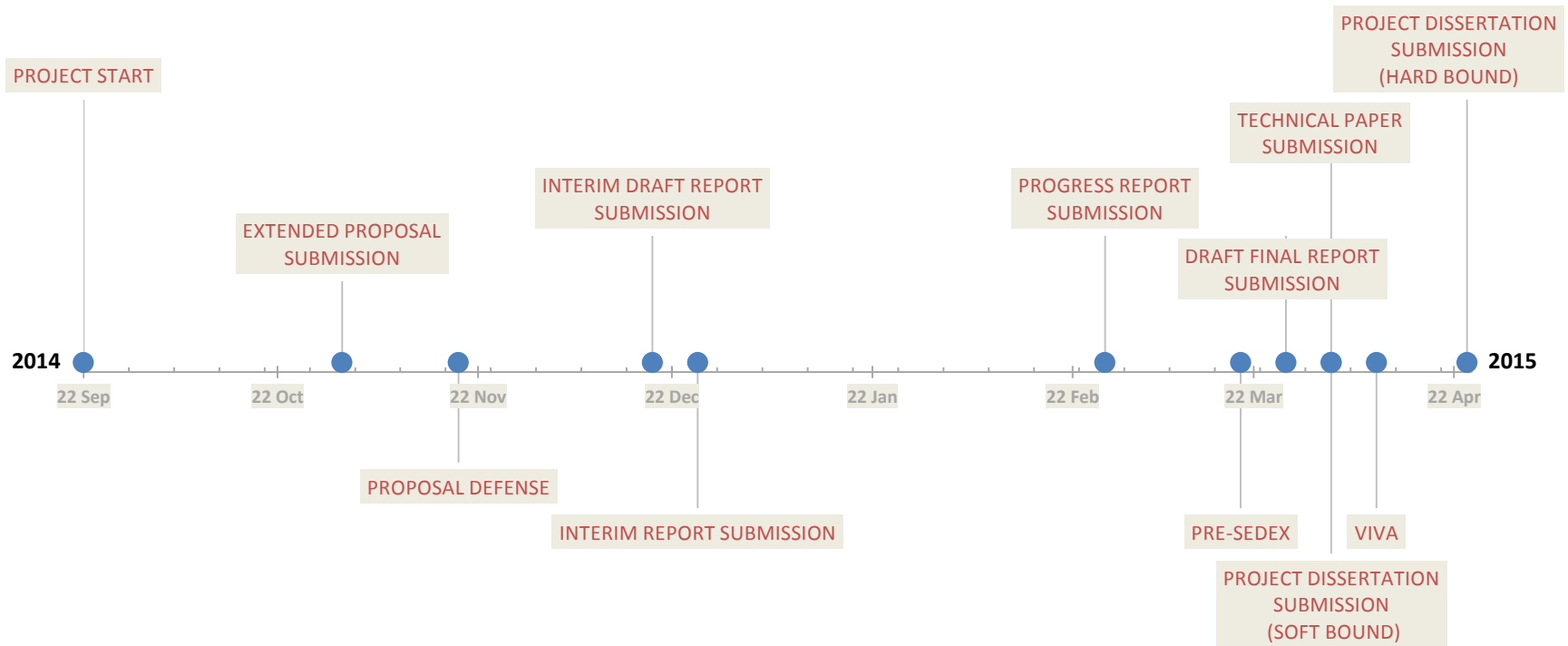
It is best to conduct the frequency scan analysis technique first when conducting harmonic resonance analysis. This is due to the fact that when there are dangerous or harmful resonant points detected, a further analysis using the harmonic resonance mode analysis technique can be made. Unlike frequency scan analysis which its peak does not always correspond to the true resonance frequency, harmonic resonance mode analysis helps to solve this drawback though providing necessary information on revealing the critical modes and the area to be affected.

REFERENCES

- [1] IEEE Task Force on Harmonics Modeling and Simulation, “Modelling and Simulation of the Propagation of Harmonics in Electric Power Networks: Part I,” *IEEE Trans. Power Del.*, vol. 11, no.1, pp. 466-474, Jan. 1996.
- [2] A. Frobel, and R. Vick, “Chosen aspects for harmonic analysis in distribution networks,” presented at 22nd International Conference and Exhibition on Electricity Distribution, June 10-13, 2013.
- [3] M. Esmaili, H. A. Shayanfar, and A. Jalilian, “Modal analysis of power systems to mitigate harmonic resonance considering load models,” *J. Energy*, vol. 33, no. 9, pp. 1361–1368, Sep. 2008.
- [4] K. N. M. Hasan, K. Rauma, P. Rodriguez, J. I. Candela, and A. Luna, “Harmonic Compensation Analysis in Offshore Wind Power Plants Using Hybrid Filters,” *IEEE Transactions on Industry Application*, vol. 50, no. 3, pp. 2050-2060, May/Jun. 2014
- [5] C. Amornvipas, and L. Hofmann, “Resonance Analyses in Transmission Systems: Experience in Germany.” in *Proc. of IEEE PES Gen. Meet.*, Jul. 25-29, 2010, pp. 1-8.
- [6] H. Zhou, Y. Wu, S. Lou, and X. Xiong, “Power System Series Harmonics Resonance Assessment Based on Improved Modal Analysis,” *IU-Journal Of Electrical & Electronics Engineering*, vol. 7, no. 2, pp. 423 – 430, 2007
- [7] A. Medina, J. Segundo, P. Ribeiro, W. Xu, K. L. Lian, G. W. Chang, V. Dinavahi, and N. R. Watson, “Harmonic Analysis in Frequency and Time Domain,” *IEEE Trans. Power Del.*, vol. 28, no. 3, pp. 1813-1821, Jul. 2013.
- [8] P. R. Nasini, N. R. Narra, and A. Santosh, “Modeling and Harmonic Analysis of Domestic/ Industrial Loads.” *International Journal of Engineering Research and Applications*, vol. 2, no. 5, pp. 485-491, Sep./Oct., 2012

- [9] IEEE Task Force on Harmonics Modeling and Simulation. Modeling and simulation of the propagation of harmonics in electric power networks: Part II,” *IEEE Trans. Power Del.*, vol. 11, no. 1, pp. 466–74, Jan. 1996
- [10] Z. Y. Huang, W. Xu and V. R. Dinavahi, “A practical harmonic resonance guideline for shunt capacitor applications,” *IEEE Trans. Power Del.*, vol. 18, pp. 1382-1387, Apr. 2003.
- [11] Z. Huang, Y. Cui, and W. Xu, “Application of modal sensitivity for power system harmonic resonance analysis,” *IEEE Trans, Power Syst*, vol. 22, no. 1, pp. 222-231. Feb. 2007.
- [12] W. Xu, Z. Y. Huang, Y. Cui, and H. Z. Wang, “Harmonic Resonance Mode Analysis,” *IEEE Trans. Power Del.*, vol. 20, pp. 1182-1190, 2005.
- [13] R. Bellman, “Introduction to Matrix Analysis”, 2nd ed. New York: McGraw-Hill, 1970
- [14] E. Acha, and M. Madrigal, “Power System Harmonics Computer Modelling and Analysis”, Chichester: Wiley, 2001

APPENDICES



Key Milestone for Final Year Project I (FYP I) & Final Year Project II (FYP II)

Gantt Chart for Final Year Project I (FYP I)

No	Activities/ Week	1	2	3	4	5	6	7	8	9	10	11	12	13	14
1	Selection of project topic	■	■												
2	Study on past research papers		■	■	■	■									
3	Discussion with SV on project and proposal draft				■	■									
4	Submission of Extended Proposal						■								
5	Preparation for Proposal Defense							■	■						
6	Proposal Defense									■					
7	Development of algorithm based on several test systems										■	■	■	■	■
8	Result gathering and analysis										■	■	■	■	■
9	Discussion with SV on results and interim draft												■	■	
10	Submission of Interim Draft Report													■	
11	Submission of Interim Report														■

Gantt Chart for Final Year Project II (FYP II)

No	Activities/ Week	1	2	3	4	5	6	7	8	9	10	11	12	13	14	15
1	Retrieve and preparation of data for UTP distribution network from GDC	■	■													
2	Development and enhancement of algorithm based on UTP distribution test systems	■	■	■	■	■	■	■								
3	Results gathering and analysis			■	■	■	■	■								
4	Discussion with SV on progress report						■	■								
5	Submission of Progress Report							■								
6	Enhancement of algorithm based on UTP distribution test systems							■	■	■						
7	Preparation for Pre-SEDEX								■	■						
8	Pre-SEDEX										■					
9	Discussion with SV on progress and final report										■	■				
10	Submission of Draft Final Report											■				
11	Submission of Project Dissertation (soft bound)												■			
12	Submission of Technical Report												■			
13	Preparation for Viva												■			
14	Viva													■		
15	Submission of Project Dissertation (hard bound)															■

Standard code used for frequency scan analysis and harmonic resonance mode analysis technique:

```

%dpi14buses.m
clear all
data14busstandard;
%data14buses;
%data14busesHVDC;
z=(h1:dh:h2)*0;
k=0;
H=linspace(1,40,118);
for h=h1:dh:h2
    Y=zeros(nN,nN);
    %
    for n=1:nL %calculate line admittance
        node1=n1(n);
        node2=n2(n);
        y12=1/(r1(n)+1i*h*x1(n));
        y00=1i*h*b2(n);
        Y(node1, node1)=Y(node1, node1)+y12+y00;
        Y(node2, node2)=Y(node2, node2)+y12+y00;
        Y(node1, node2)=Y(node1, node2)-y12;
        Y(node2, node1)=Y(node2, node1)-y12;
    end
    %}
    %
    for n=1:nG %calculate admittance at the generators
        node1=ng(n);
        yg=1/(1i*h*xg(n));
        Y(node1, node1)=Y(node1, node1)+yg;
    end
    %}
    %
    for n=1:nN %calculate load admittance
        node1=nn(n);
        if PL(n)~=0;
            R=V(n)^2/PL(n); %CIGRE load model (i) and (iii)
            %R=(V(n)^2)/((0.1*h+0.9)*PL(n)); %CIGRE load model (ii)
            %Xl=(j*h*V(n)^2)/QL(n); %CIGRE load model (i)
            %Xl=(j*V(n)^2)/((0.1*h+0.9)*QL(n)); %CIGRE load model (ii)
            Xl=1i*h*R/(6.7*(QL(n)/PL(n)-0.74)); %CIGRE load model
            (iii)
            Xs=1i*h*0.073*R; %CIGRE load model (iii)
            %yl=1/(R*Xl/(R+Xl)); %CIGRE load model (i) and (ii)
            yl=1/(R*Xl/(R+Xl)+Xs); %CIGRE load model (iii)
            Y(node1, node1)=Y(node1, node1)+yl+Yc(n);
        end
    end
    %}
    %
    %{
    %%calculate filter admittance
    for n=1:nN
        node1=nn(n);

```

```

if rf(n)~=0;
    Xf=j*h*xf(n);
    Xc=j*h*bf(n);
    yf=(1/(rf(n)+Xf))+Xc;
    Y(nodel1, nodel1)=Y(nodel1, nodel1)+yf;
end
end
%}
k=k+1;
%HRMA starts here
[L,D] = eig(Y); %compute D (eigenvalue) and L (left eigenvector)
R=inv(L); %compute R (right eigenvector)
Y=L*D*R; % check L*D*R = Y
Zm=pinv(D);
%zm11(k)=Zm(1,1);
%zm11=abs(zm11);
%zm1414(k)=Zm(14,14);
%zm1414=abs(zm1414);
%
zm11(k)=Zm(1,1);
zm11=abs(zm11);
zm22(k)=Zm(2,2);
zm22=abs(zm22);
zm33(k)=Zm(3,3);
zm33=abs(zm33);
zm44(k)=Zm(4,4);
zm44=abs(zm44);
zm55(k)=Zm(5,5);
zm55=abs(zm55);
zm66(k)=Zm(6,6);
zm66=abs(zm66);
zm77(k)=Zm(7,7);
zm77=abs(zm77);
zm88(k)=Zm(8,8);
zm88=abs(zm88);
zm99(k)=Zm(9,9);
zm99=abs(zm99);
zm1010(k)=Zm(10,10);
zm1010=abs(zm1010);
zm1111(k)=Zm(11,11);
zm1111=abs(zm1111);
zm1212(k)=Zm(12,12);
zm1212=abs(zm1212);
zm1313(k)=Zm(13,13);
zm1313=abs(zm1313);
zm1414(k)=Zm(14,14);
zm1414=abs(zm1414);
%}
%frequency scan analysis starts here
Z=pinv(Y);
%z44(k)=Z(4,4);
%z44=abs(z44);
%z1414(k)=Z(14,14);
%z1414=abs(z1414);

```

```

z11(k)=Z(1,1);
z11=abs(z11);
z22(k)=Z(2,2);
z22=abs(z22);
z33(k)=Z(3,3);
z33=abs(z33);
z44(k)=Z(4,4);
z44=abs(z44);
z55(k)=Z(5,5);
z55=abs(z55);
z66(k)=Z(6,6);
z66=abs(z66);
z77(k)=Z(7,7);
z77=abs(z77);
z88(k)=Z(8,8);
z88=abs(z88);
z99(k)=Z(9,9);
z99=abs(z99);
z1010(k)=Z(10,10);
z1010=abs(z1010);
z1111(k)=Z(11,11);
z1111=abs(z1111);
z1212(k)=Z(12,12);
z1212=abs(z1212);
z1313(k)=Z(13,13);
z1313=abs(z1313);
z1414(k)=Z(14,14);
z1414=abs(z1414);
end
%plotting Frequency Scan Analysis graph
subplot(2,1,1);
%plot(H,z1414);
plot(H,z11,H,z22,H,z44,H,z55,H,z99,H,z1111,H,z1414);
%plot(H,z11,H,z22,H,z44,H,z55,H,z88);
axis([0,40,0,40]);
title('Frequency Scan Analysis of the Modified 14 Bus Test System');
xlabel('Harmonic');
ylabel('Magnitude [p.u.]');
legend
('Bus1','Bus2','Bus3','Bus4','Bus5','Bus6','Bus7','Bus8','Bus9','Bus10',
'Bus11','Bus12','Bus13','Bus14');
grid on;
%plotting Harmonic Resonance Mode Analysis graph
subplot(2,1,2);
%plot(H,zm1414);
plot(H,zm11,H,zm22,H,zm33,H,zm44,H,zm55,H,zm66,H,zm77,H,zm88,H,zm99,H,
zm1111,H,zm1212,H,zm1313,H,zm1414);
axis([0,40,0,40]);
title('Harmonic Resonance Mode Analysis of the Modified 14 Bus Test
System');
xlabel('Harmonic');
ylabel('Magnitude [p.u.]');legend
('Mode1','Mode2','Mode3','Mode4','Mode5','Mode6','Mode7','Mode8','Mode
9','Mode10','Mode11','Mode12','Mode13','Mode14');grid on;

```